States and stability of the climate system

We have seen that the climate system is a complex association of interacting components, each having an intrinsic time scale. These interactions give rise to positive and negative feedbacks.

Positive feedbacks are such that an initial perturbation of the system is amplified through the interactions.

Negative feedbacks, on the other hand, damp an initial perturbation.

This complexity calls for a multitude of possible states of the climate system. In this context we may ask:

- How many possible states are there?
- How stable are the different states?
- How does the system move from one state to the next?

Abrupt climate changes

There is increasing evidence that abrupt climate changes have occurred in the past. One of the best-studied and well-known examples is the Younger Dryas (Alley, 2000; Broecker, 2003). The Younger Dryas was a millenium-long cold snap that occurred in the transition from the last glacial time and the Holocene.

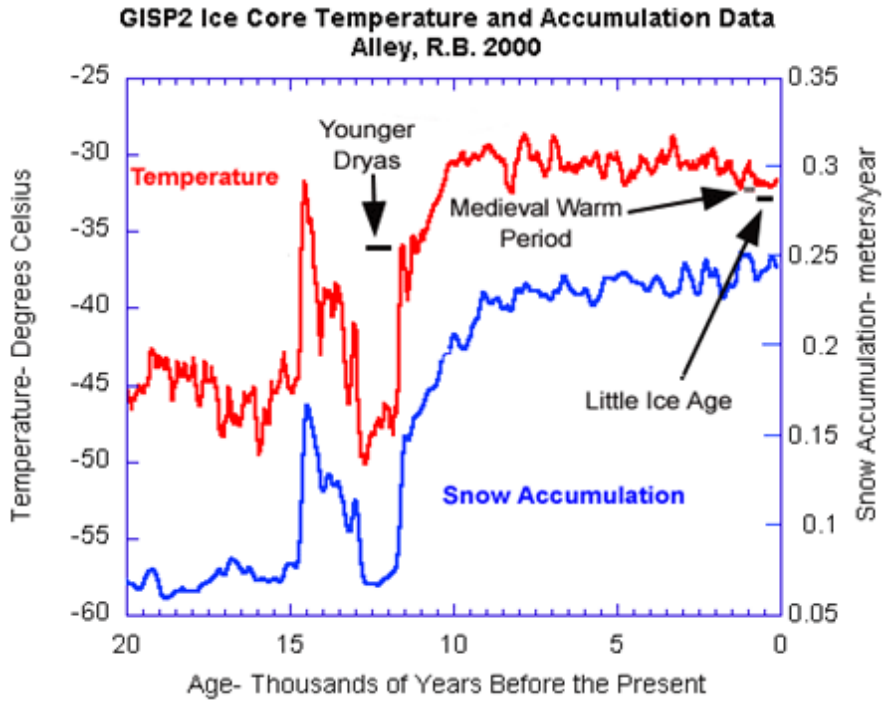

Alley, R.B., 2000: The Younger Dryas cold interval as viewed from central Greenland. Quaternary Science Reviews, 19 (1-5), 213-226.

Broecker, W.S., 2003: Does the Trigger for Abrupt Climate Change Reside in the Ocean or in the Atmosphere? Science, 300, 1519-1522.

Causes of the Younger Dryas

Broecker (2003) states that: ‘The prevailing view of this cold snap is that it was triggered by a catastrophic release of fresh water stored in proglacial Lake Agassiz. This release was initiated when the retreating margin of the Laurentide ice sheet opened a lower outlet, allowing much of the lake’s stored water to flood across the region now occupied by the northern Great Lakes into the St. Lawrence valley and from there into the northern Atlantic. On the basis of reconstructions of the pre- and postdiversion shorelines of Lake Agassiz, it has been estimated that 9500 km^3 of water was released. If released over the course of a single year, this flood would match today’s net annual input of fresh water to the Atlantic Ocean region north of 45°N. “

In most ocean models, an input of this magnitude cripples formation of deep water in the northern Atlantic (i.e., it greatly weakens or even shuts down the model’s conveyor circulation).’

Possible causes for the Younger Dryas

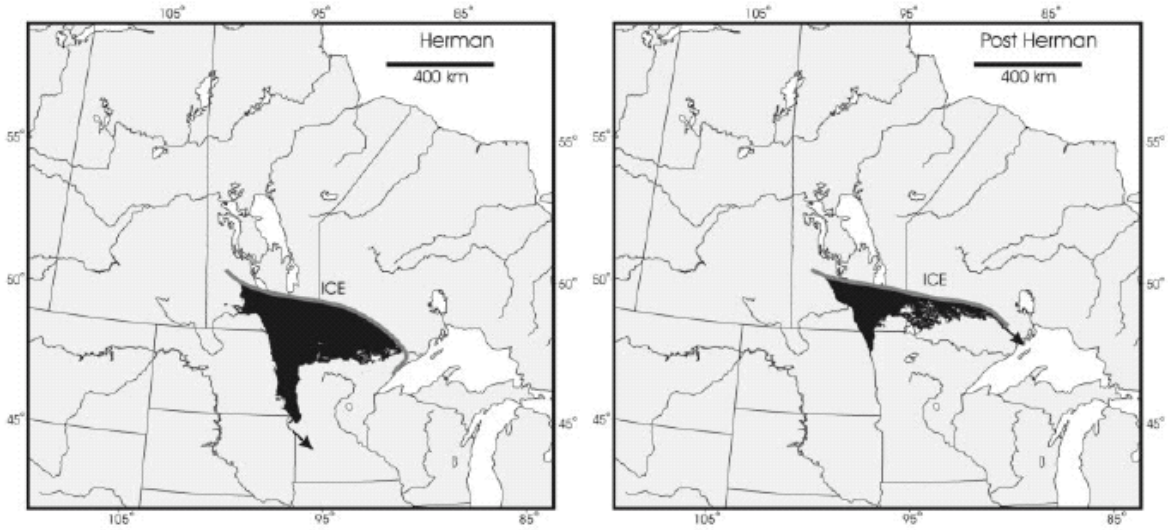

Fig. 1. (**Left**) The outline of Lake Agassiz just before the catastrophic flood. At that time its outlet was to the south into the Mississippi drainage. (**Right**) The outline after the opening of the eastward outlet. A volume of 9500 km³ of water was suddenly released to the northern Atlantic through the St. Lawrence Valley (*42*).

Broecker (2003)

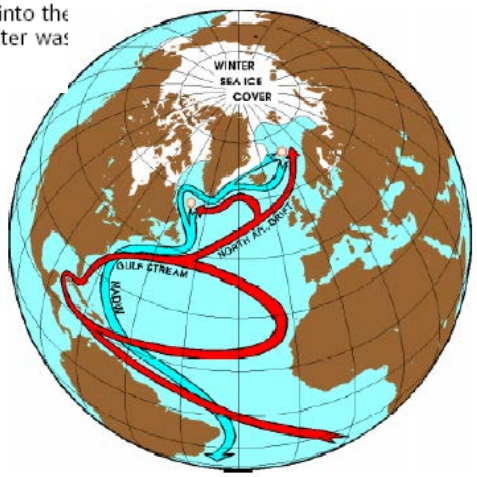

Fig. 3. The Atlantic Conveyor Belt. Orange circles show the regions of convection in the Greenland/Norwegian and Labrador Seas. The outflow of North Atlantic Deep Water (NADW) is shown in blue.

Rahmstorf (1999)

The Younger Dryas is Switzerland

Sediment cores in lakes, for example in Gerzensee, show changes in the ratios of oxygen isotopes (recording temperature) in parallel to the ice cores in Greenland. This provides evidence that the abrupt Younger Dryas cooling event was of regional if not hemispheric scale.

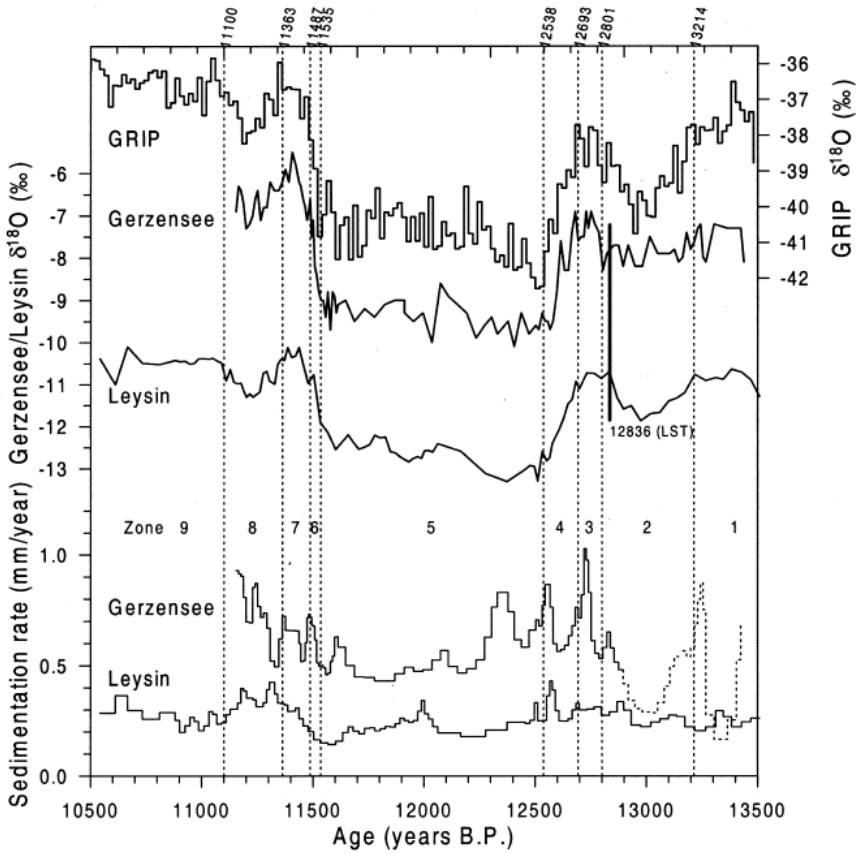

Fig. 4. Correlation between the $\delta^{18}O$ curves of Gerzensee, Leysin, and GRIP and inferred sedimentation rates for the lake cores. The age scale in calendar years before present (present is 1950 A.D.). Numbers indicated in the upper part of the figure are ages of isotopic zone boundaries. The dashed line in the Gerzensee sedimentation record indicates poor matching.

A series of abrupt climate changes

The ice-core records from Greenland reveal that abrupt climate events (warm ‘Dansgaard-Oeschger’ events and cold ‘Heinrich’ events) have occurred several times in the past. There is some evidence that these changes were induced by marginal instability of the ‘warm-mode’ North Atlantic circulation and massive fresh-water discharges (icebergs) into the North Atlantic.

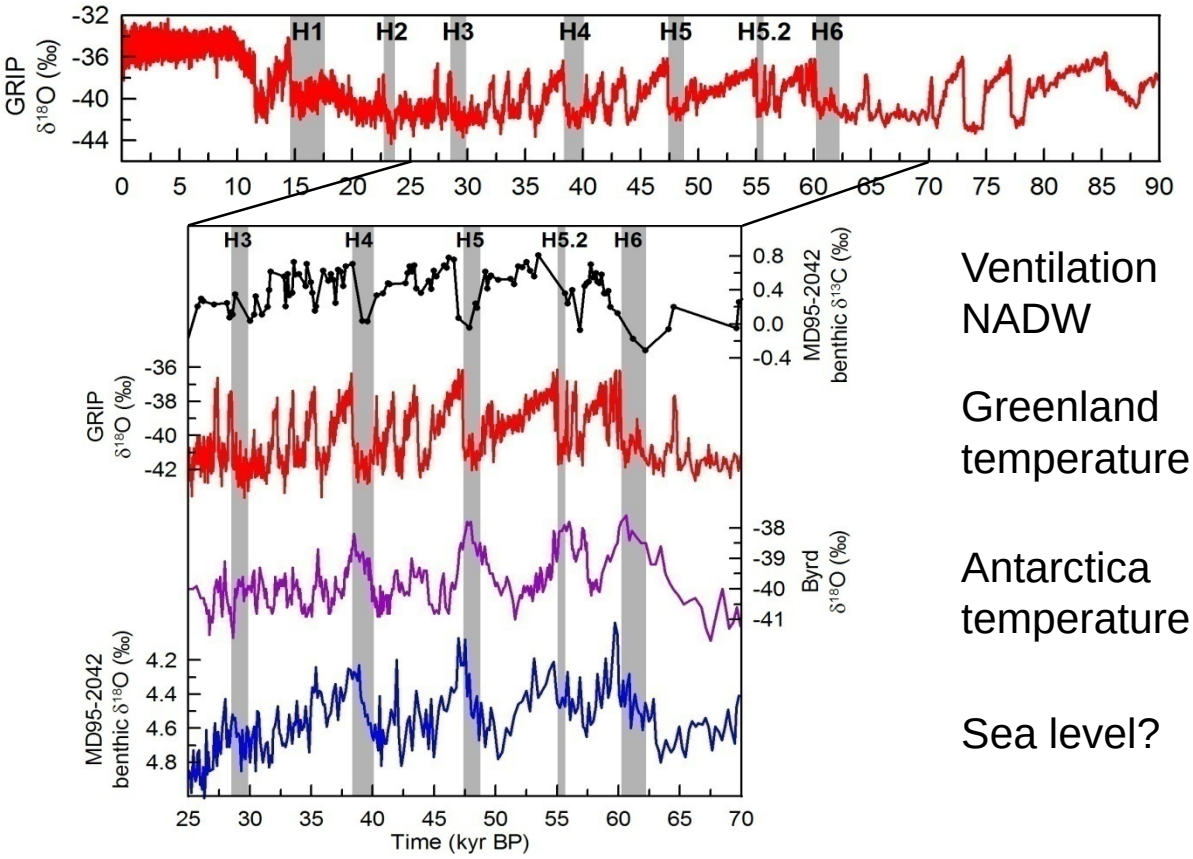

Ventilation NADW

Greenland temperature

Antarctica temperature

Sea level?

Spatial extent of abrupt events

Events of the kind of the Younger Dryas are generally not confined to a limited area but have global reach (Broecker, 1997).

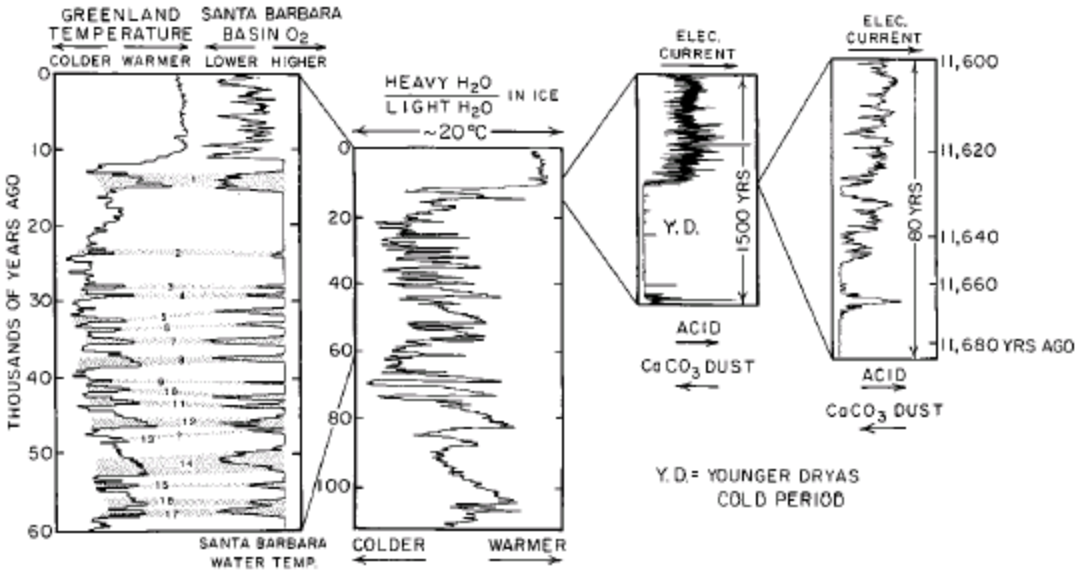

Fig. 3. As shown in the center panel, the oxygen isotope record from the Summit Greenland ice cores (GRIP and GISP2) clearly demonstrates that except for the last 10,000 years, the last 110,000 years were punctuated by large and abrupt climate changes (*1*). As shown in the left-hand panel, these same changes appear in the marine record from the Santa Barbara Basin as alternations between periods of vigorous and sluggish ventilation (*35*). The large and abrupt changes in electrical conductivity shown in the right-hand panel reflect shifts from intervals of extreme cold when the influx of $CaCO_3$-bearing dust greatly exceeded that of proton-bearing acids to warmer intervals when this onslaught of dust from Asia was stemmed (*22*). The blowup portrays that these shifts were not only abrupt but quite noisy. Taken together, this evidence suggests that Greenland air temperatures, Asian winds, and northern Pacific surface salinities underwent large and synchronous changes that were accomplished on the time scale of a few decades (*55*). The flickering action associated with these transitions could cause havoc in agricultural production were another such change to occur 100 or so years from now.

Synchrony of abrupt events

In agreement with the concept of a bipolar seesaw, a shift in the ocean circulation often results in an antiphase relation between the two hemispheres.

When the thermohaline circulation is strong (top), it is generally warm and wet in the north and cool in the south. When the THC is weak or off, it is cold and dry in the north and warmer in the south (bottom). From Rahmstrorf, Nature 2002.

Reconstructed temperature shifts can exceed 15°C in a few decades in Greenland.

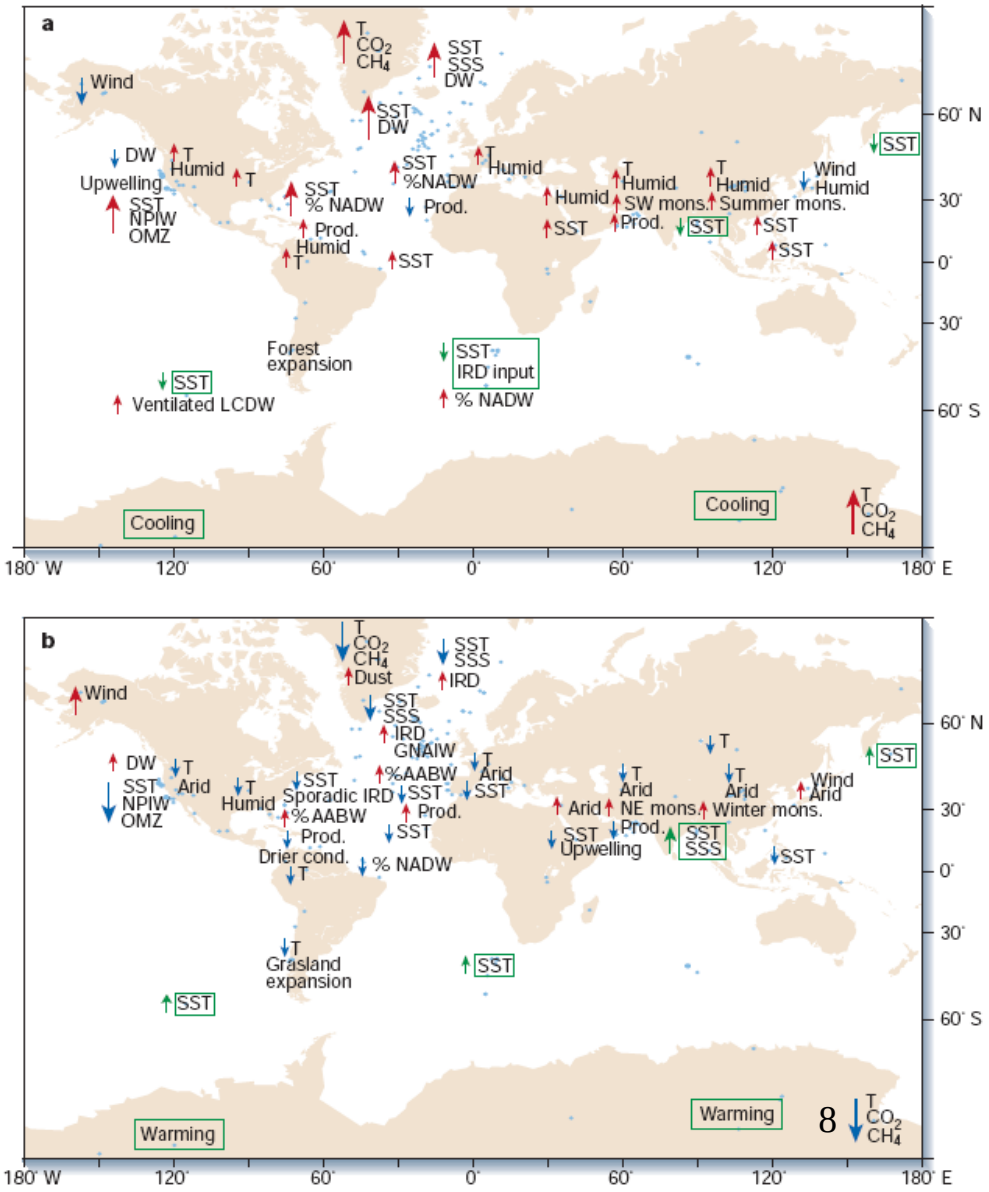

How abrupt?

Changes in isotopic and chemical compositions in Greenland ice cores show a shift within a few years during abrupt climate events. Climate models show transitions that take a few tens to a hundred years to complete.

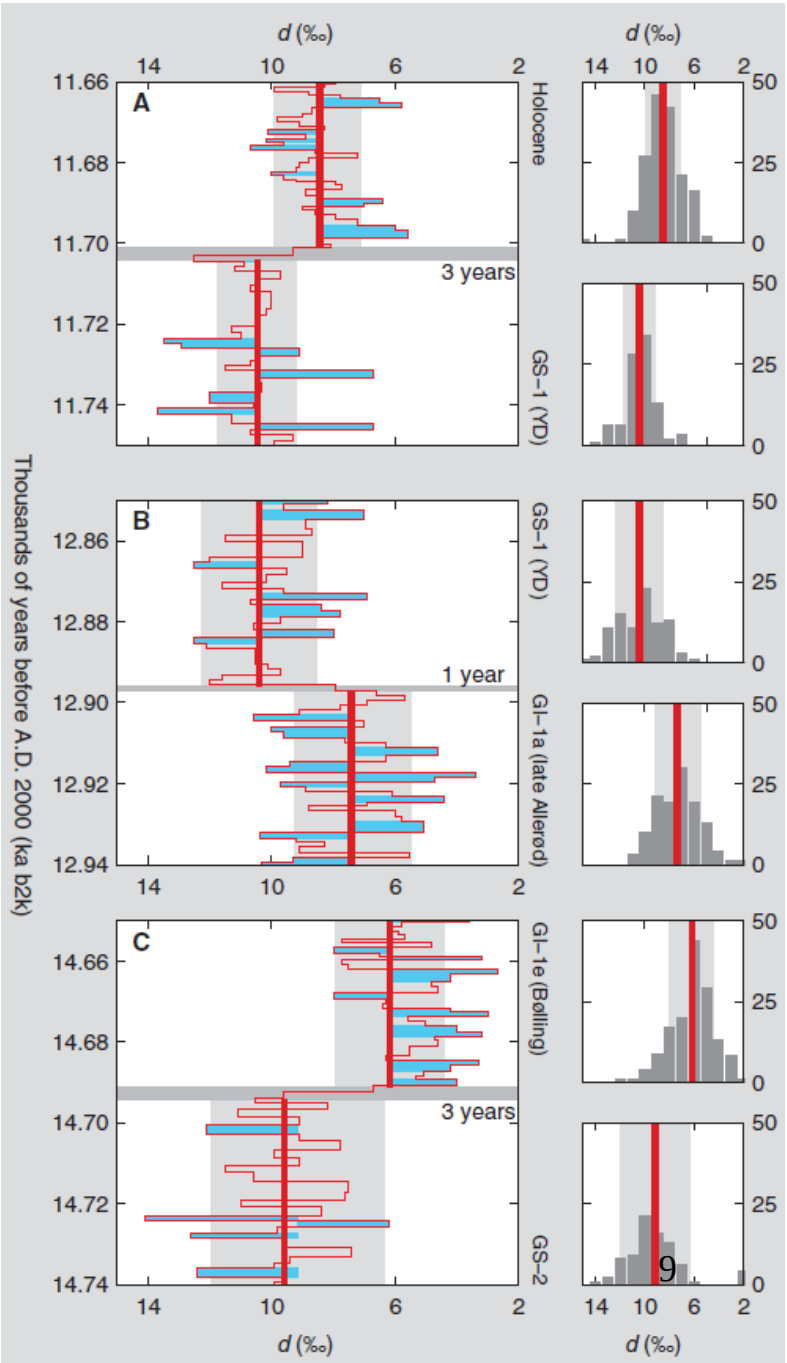

Modelling of abrupt events

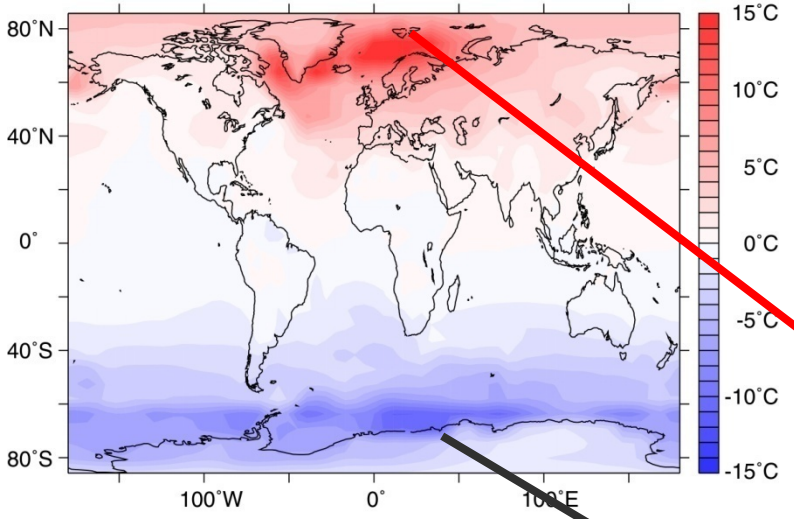

Temperature difference
"THC on" - "THC off"

(ECBILT-CLIO model)

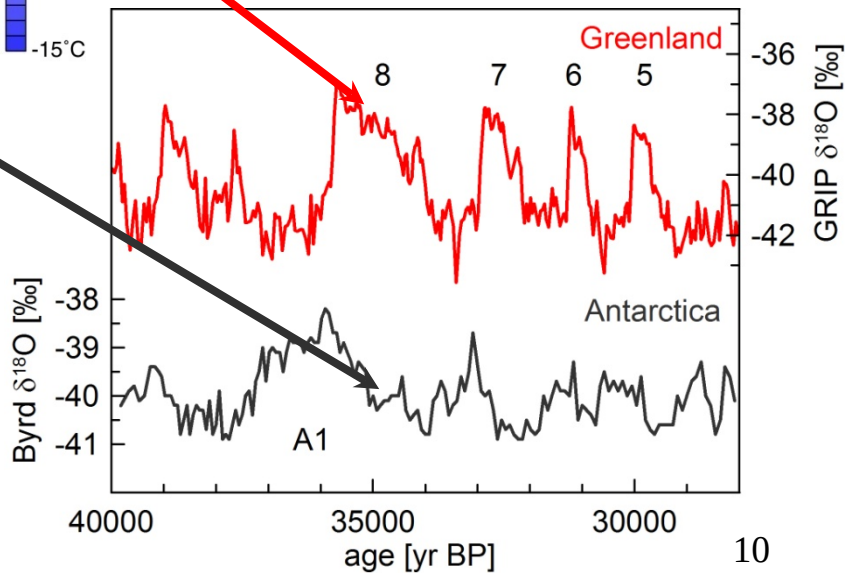

Temperature proxy data from Greenland and Antarctica

The hysteresis behaviour of the thermohaline circulation

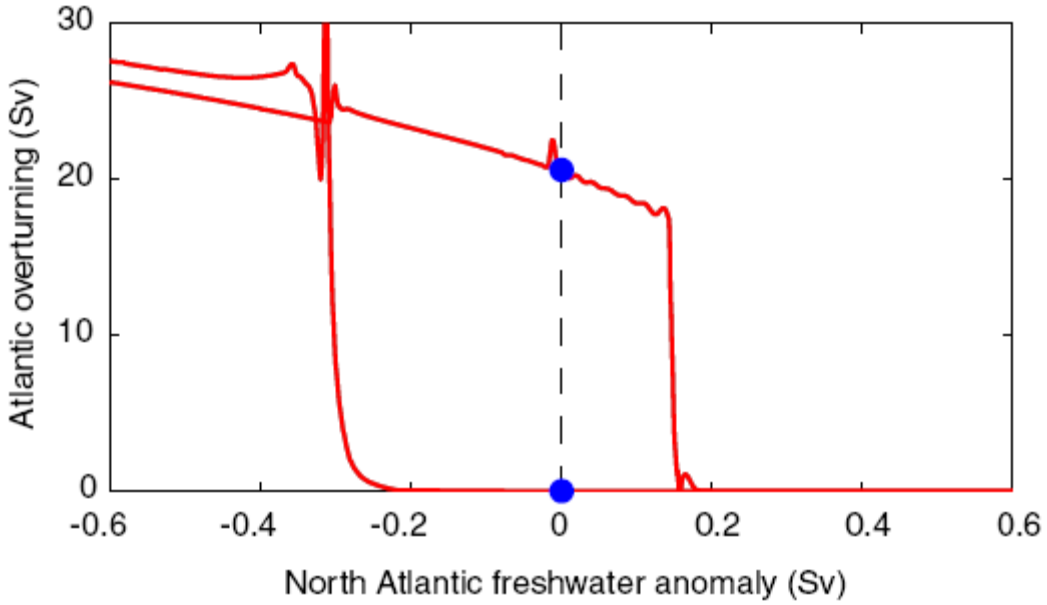

Hystersis loop in the Bern2.5D climate model, in a simulation where freshwater forcing in the North Atlantic was increased and then decreased very slowly. The two blue points are the two stable without forcing of an ocean with and one without thermohaline circulation in that particular model.

The hysteresis behaviour of the thermohaline circulation

Depending on the position of the system in the hysteresis loop and the amplitude of the perturbation, a transition can be a) linear, reversible, b) nonlinear, reversible or c) nonlinear, irreversible. From Stocker and Marchal, PNAS 2000.

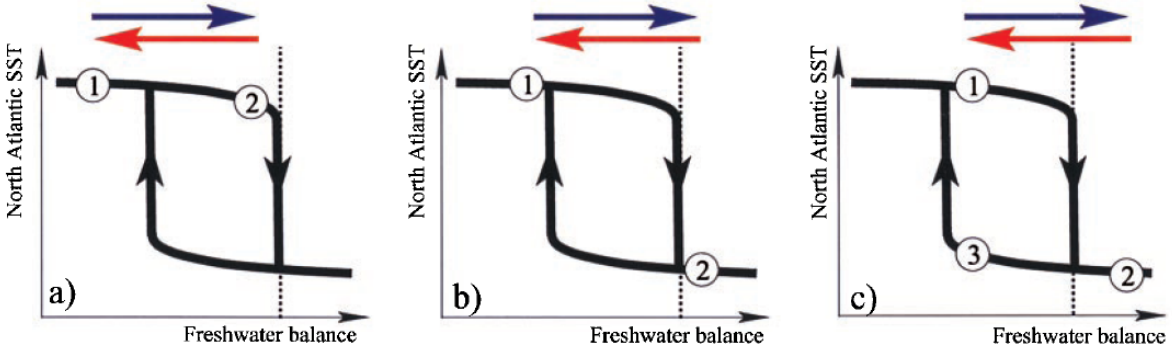

Fig. 1. The ocean–atmosphere system is a nonlinear physical system that can exhibit hysteresis behavior (13). The upper branch of the hysteresis is characterized by warm North Atlantic sea surface temperatures (SST), the lower branch by cold sea surface temperatures. A given perturbation (indicated by the blue and red arrows) in the freshwater balance of the North Atlantic (precipitation + runoff − evaporation) causes transitions from an initial state *1* to states *2* and/or *3*. Three structurally different responses are possible depending on whether threshold values (dashed line) are crossed: (*a*) Linear, reversible response. (*b*) Nonlinear, reversible response. (*c*) Nonlinear, irreversible response.

Climate change and human civilization

More recent abrupt shifts in the global or regional climate had profound impacts on human civilization (Mesopotamia, 4200 B.P.; Yucatan, 1200 B.P.), as documented in a study by deMenocal (2001).

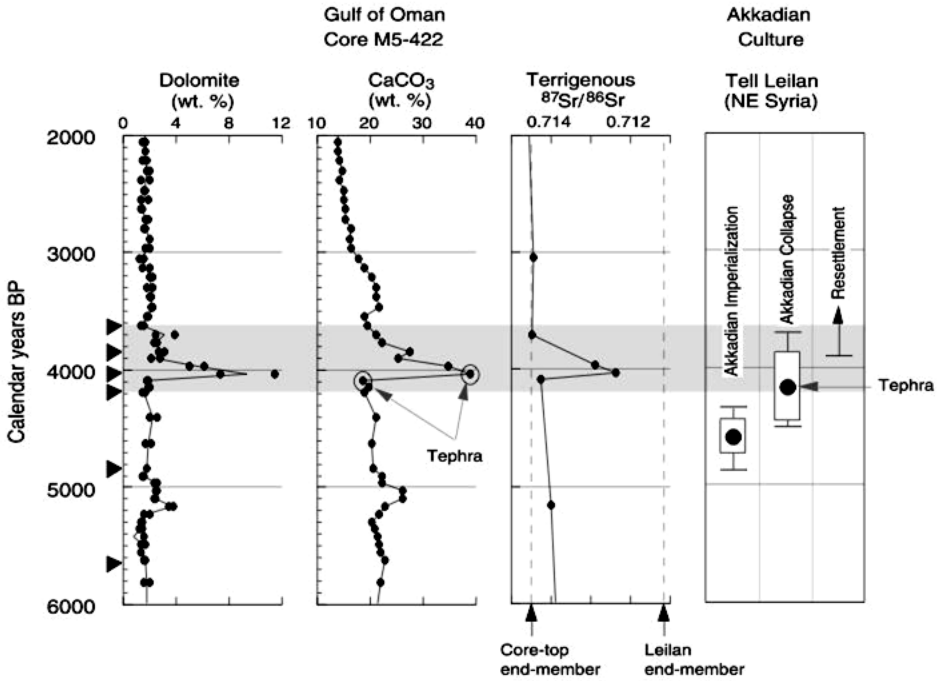

Fig. 4. Mesopotamian paleoclimate and the collapse of the Akkadian empire.

Fig. 3. Excavated sample of residential occupation (600 m^2) within the lower town of Tell Leilan, northeast Syria (100 ha), during the terminal Akkadian empire occupation. Abrupt climate change (ca. 2200 B.C.) forced the Akkadian abandonment of rain-fed agriculture plains of northern Mesopotamia. [Photo credit: H. Weiss/Yale University]

Fig. 4. Mesopotamian paleoclimate and the collapse of the Akkadian empire. Detailed radiocarbon dates of archaeological remains at Tell Leilan, northeast Syria, document the abandonment and incipient collapse of the Akkadian empire near 4170 ± 150 calendar yr B.P. (*37*). A late Holocene record (*40*) of Mesopotamian aridity was reconstructed by quantifying wind-borne sediment components in a deep-sea sediment core from the Gulf of Oman, which is directly downwind of eolian dust source areas in Iraq, Kuwait, and Syria. The severalfold increase in eolian dolomite and calcite commencing at 4025 ± 125 calendar yr B.P. reflects an ~300-year interval of increased Mesopotamian aridity. A Mesopotamian provenance for this dust peak is indicated from detrital (mineral) fraction Sr (and Nd) isotopic analyses, which show a marked shift toward the measured Mesopotamian (Tell Leilan abandonment) composition (*40*). Solid triangles indicate calibrated calendar ages of radiocarbon dates on monospecific planktonic foraminifera.

deMenocal, P.B., 2001: Cultural responses to climate change during the late Holocene, Science, 292, 667-673.

Climate change and human civilization (2)

Fig. 5. Structures emerge from the surrounding tropical forest at the Maya archaeological site of Tikal in Petén, Guatemala. At its peak in the Late Classic period (ca. 800 A.D.), this urban center in the southern Maya lowlands supported ~60,000 inhabitants. It was largely depopulated after the ninth-century A.D. demographic collapse. [Photo credit: M. Brenner]

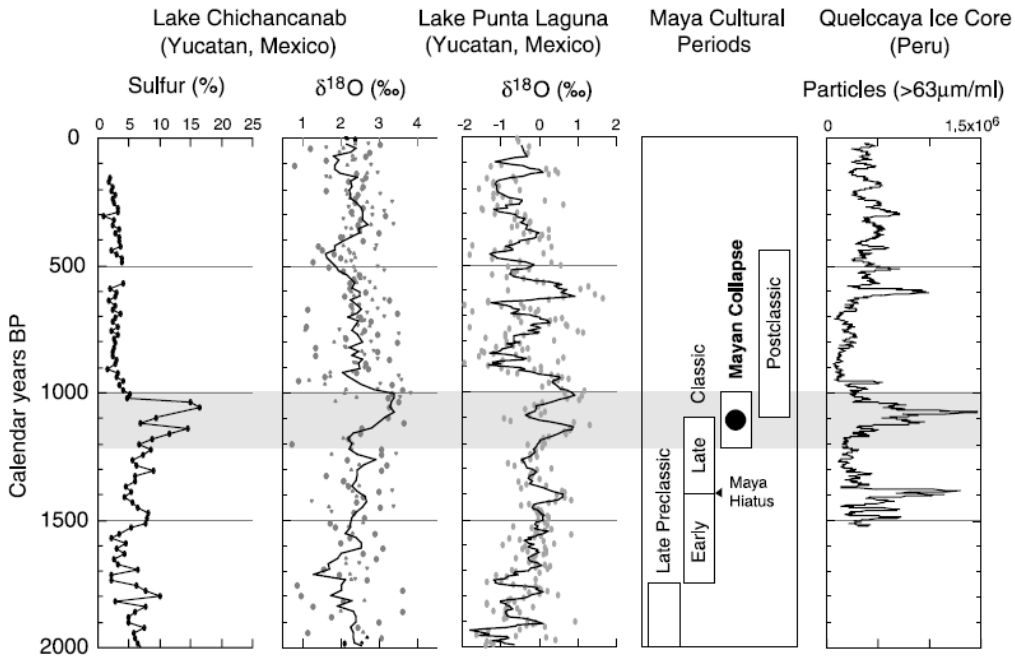

Fig. 6. Mesoamerican paleoclimate and the Classic Maya collapse. Incipient collapse of the Classic Maya civilization began near 750 to 790 A.D., and the last Maya stela or monument construction has been dated at 909 A.D. on the basis of Maya Long Count inscriptions (*44*, *45*). Well-dated sediment cores from Lakes Chichancanab (*50*) and Punta Laguna (*51*) (northern Yucatán Peninsula, Mexico) document an abrupt onset of more arid conditions spanning ~200 years between 800 and 1000 A.D., as evidenced by more evaporative (higher) $\delta^{18}O$ values and increases in gypsum precipitation (elevated sulfur content) (highlighted by gray bar through all panels). A century-long dry period coincides with the Maya Hiatus centered near 580 A.D., which documents a period (530 to 650 A.D.) of marked curtailed monument construction (*44*, *45*, *48*). Wind-borne particle concentrations from the annually dated Quelccaya ice core in the Peruvian altiplano are also shown (*53*).

deMenocal (2001)

Climate change and human civilization

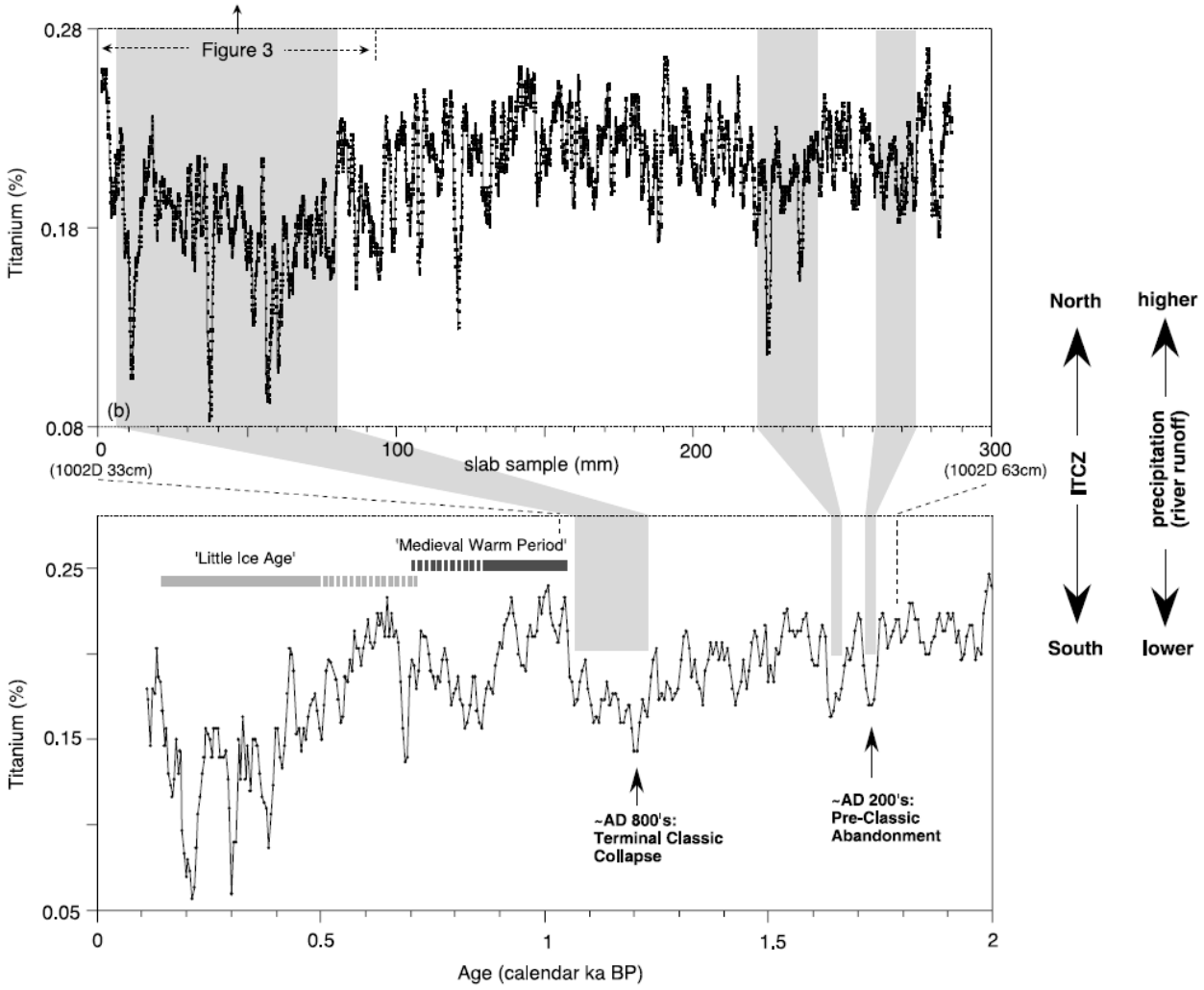

Fig. 2. (**Bottom**) Bulk Ti content [three-point running mean of 2-mm resolution measurements (*4*)] at ODP hole 1002C in the Cariaco Basin during the past 2000 years. The timing of well-known climate events (such as the Little Ice Age) and major events in the history of Maya civilization are shown. The Pre-Classic abandonment and the Terminal Classic Collapse of Maya culture coincided with phases of low riverine-derived Ti input to the Cariaco Basin and with inferred dry conditions in the region. (**Top**) The bulk Ti content (30-point running mean of 50-μm resolution analyses) of a 30-cm-long slab sample from companion ODP hole 1002D in the time interval from about 1.8 to 1.0 thousand years ago confirms these trends and shows increased detail. Periods of drought, marked by low Ti values in the sediments, are likely the result of climatic conditions that prevented the ITCZ and its associated rainfall from penetrating as far north as normal.

Haug et al. Science 2003

Extreme climatic shifts

Changes induced by a modification of some boundary condition with amplification through positive feedbacks may become extreme. Hoffman, Schrag and coworkers (2000, 2002) have postulated that a complete reversal of climate with a global glaciation ('snowball Earth') may have occurred four times between 750 and 580 millions years ago. Note that the theory is not univerally accepted.

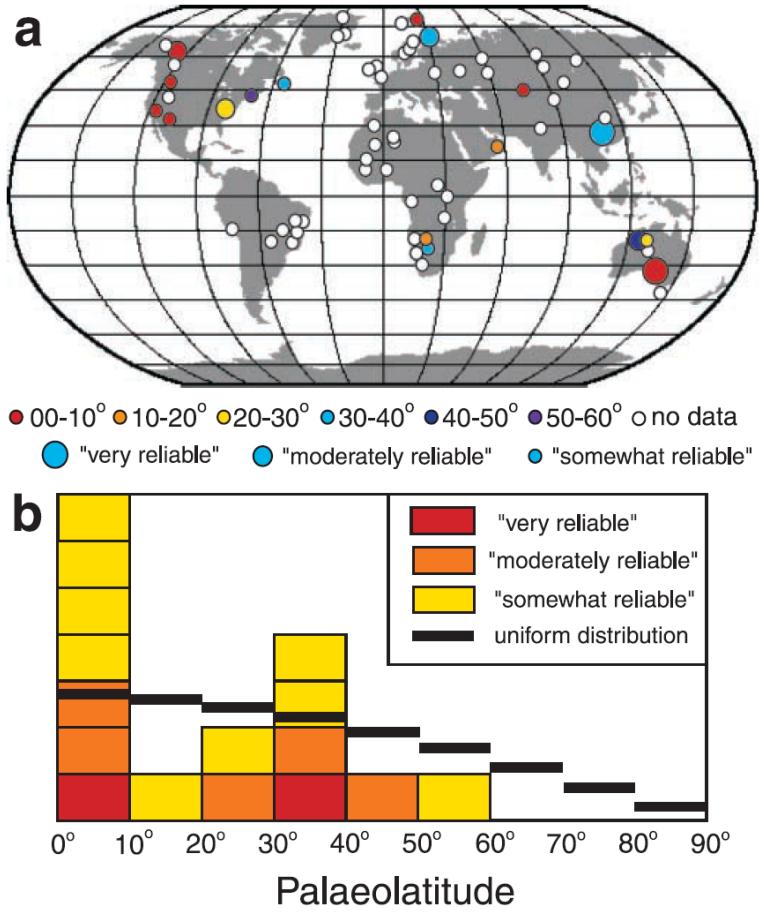

Fig. 1 Global distribution (a) of Neoproterozoic glaciogenic deposits with estimated palaeolatitudes based on palaeomagnetic data (modified from Evans, 2000). 'Reliability' takes into account not only palaeomagnetic reliability but also the confidence that the deposits represent regionally significant, low-elevation ice sheets (Evans, 2000). Histogram (b) of the same glaciogenic deposits according to palaeolatitude. The discontinuous steps show the expected density function of a uniform distribution over the sphere. Note the preponderance of low-latitude deposits and absence of high-latitude deposits. This finding would not be invalidated by plausible non-diplole components of the field, which would effectively raise the palaeolatitudes of only the mid-latitude results (Evans, 2000). The minimum in the distribution in the subtropics may reflect the meridional variation in precipitation minus evaporation due to the Hadley cells.

Hoffman, P.F. and D.P. Schrag: Snowball Earth. Scientific American, January 2000, 68-75.

Hoffman, P.F. and D.P. Schrag, 2002: The snowball Earth hypothesis: testing the limits of global change. Terra Nova, 14, 129–155.

Snowball Earth (1)

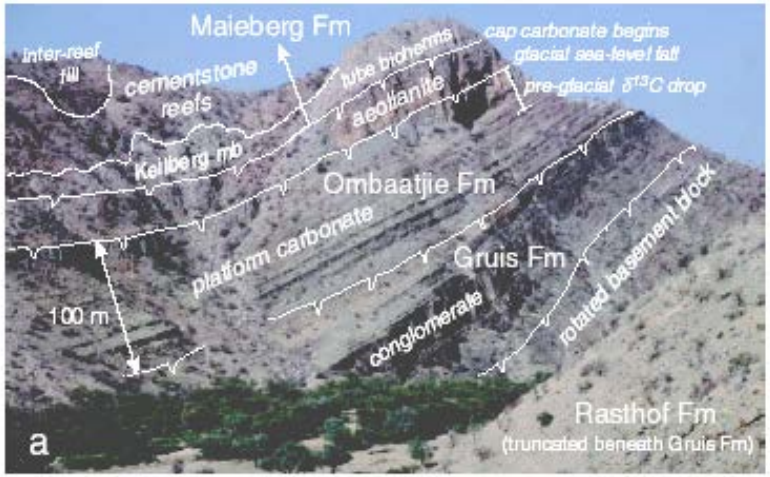

Hoffman and Schrag (2002)

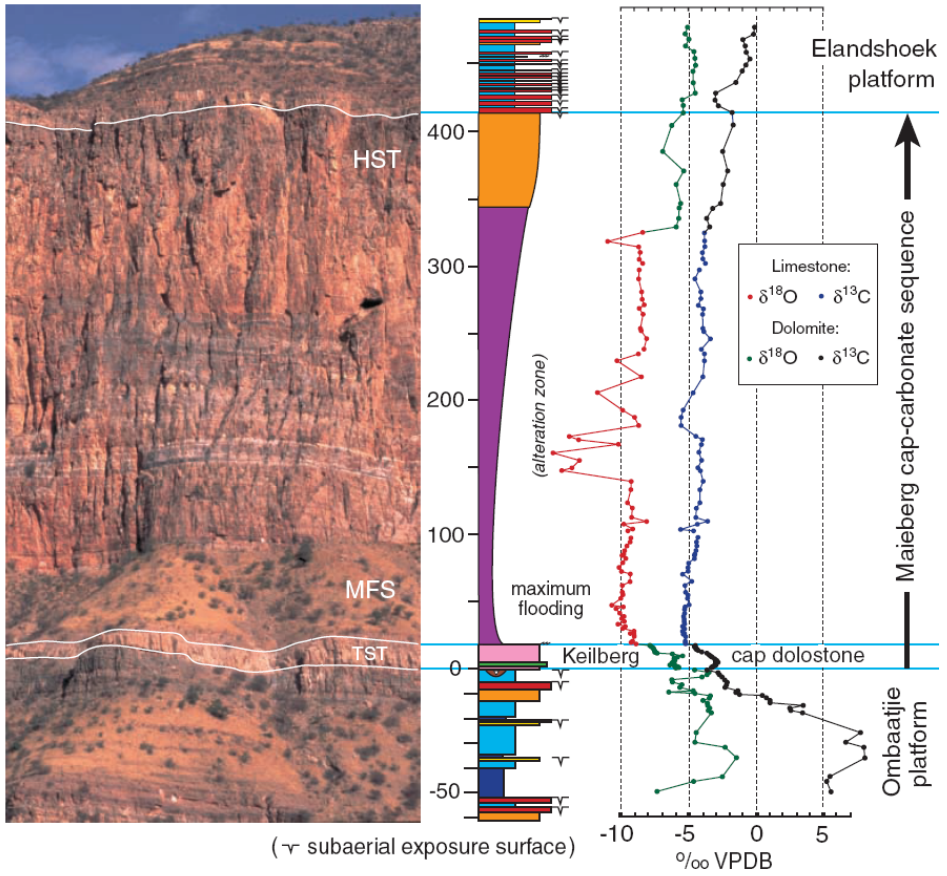

Fig. 9 New representative $\delta^{18}O$ and $\delta^{13}C$ profiles for carbonates bounding the Ghaub (Table 1) glacial surface on the Otavi platform (Khowarib Schlucht section) in northern Namibia. Pockets of diamictite occur sparingly on the glacial surface overlain by the Keilberg cap dolostone. High $\delta^{13}C$ values > 5‰ prevail for ~ 460 m beneath the preglacial drop, which is erosionally truncated in this section compared with that shown in Fig. 8(e). Section was measured and collected on the back side of the ridge shown, where the recessive interval of maximum flooding is continuously exposed. Change in scale at the datum is necessitated by the photographic perspective. Lithofacies as in Fig. 8.

Snowball Earth (2)

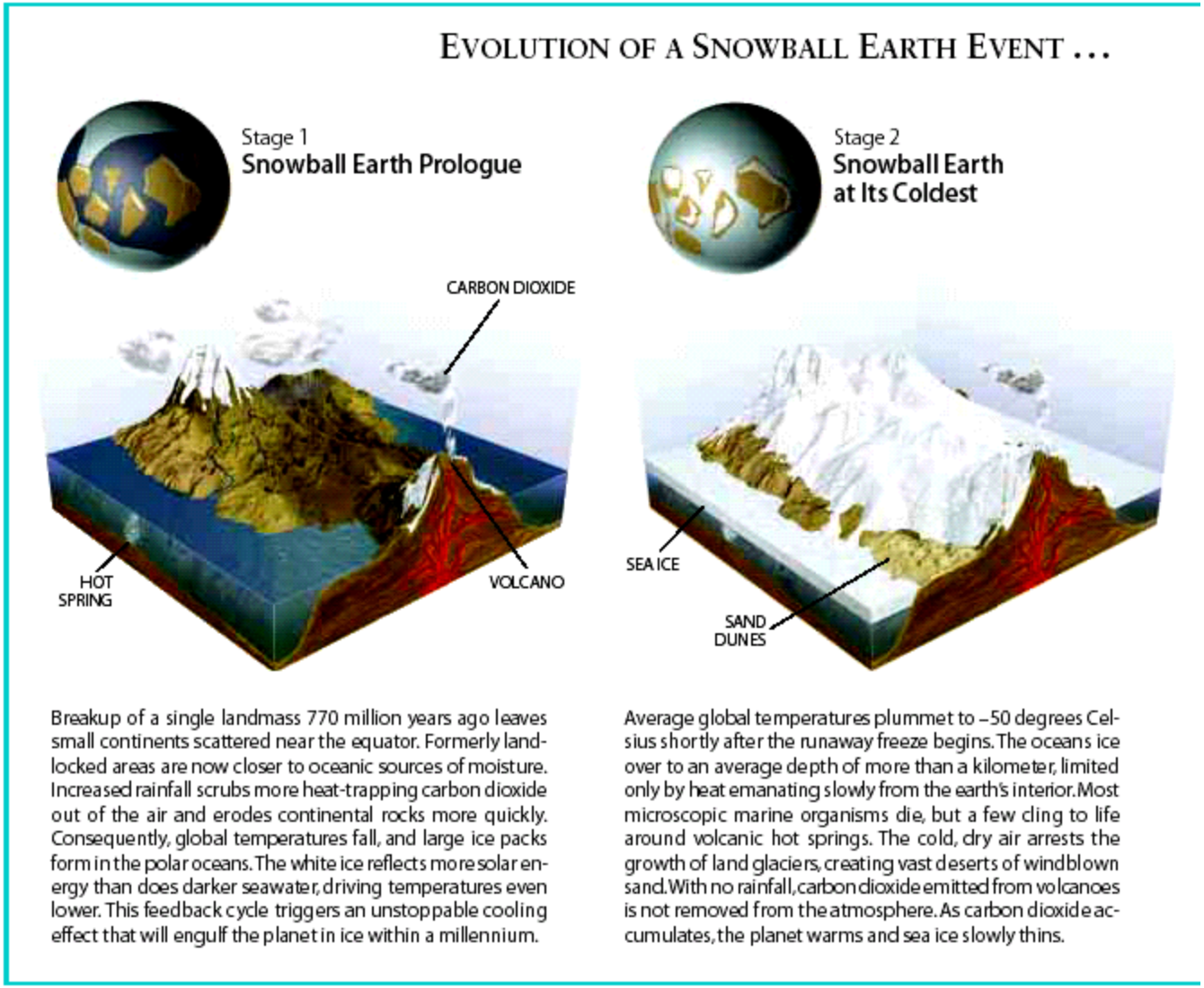

Hoffman and Schrag (2000)

Snowball Earth (2)

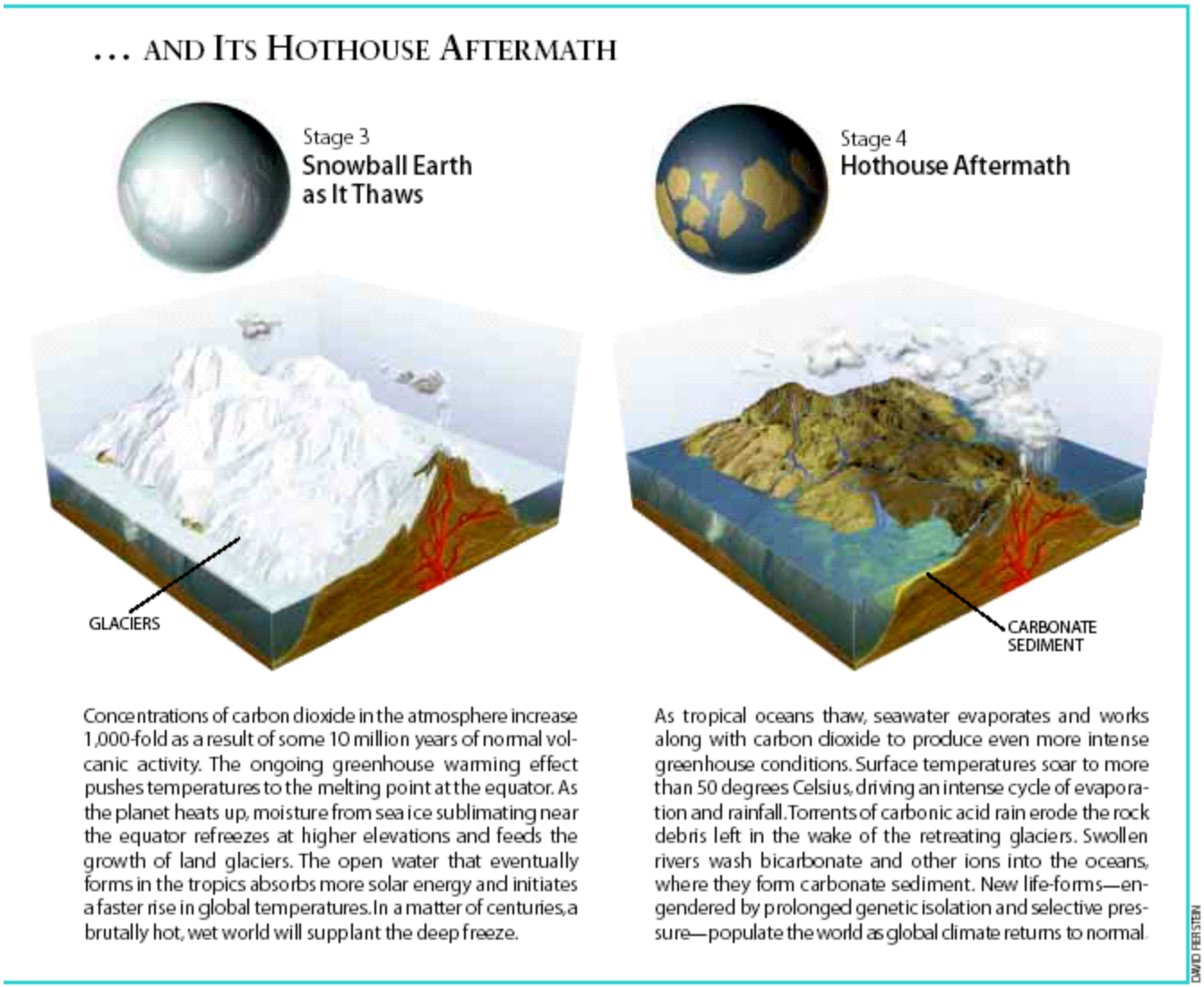

Hoffman and Schrag (2000)

Runaway climate transition

It is currently believed that extreme shifts in the state of the climate systems are associated to so-called '<u>runaway transitions</u>'. In the case of Snowball Earth we have:

more snow → lower temperature → more snow → lower temperature ...

Another example is the <u>runaway greenhouse effect</u> that may have occurred on <u>Venus</u>, explaining the absence of water on Earth's sister planet.

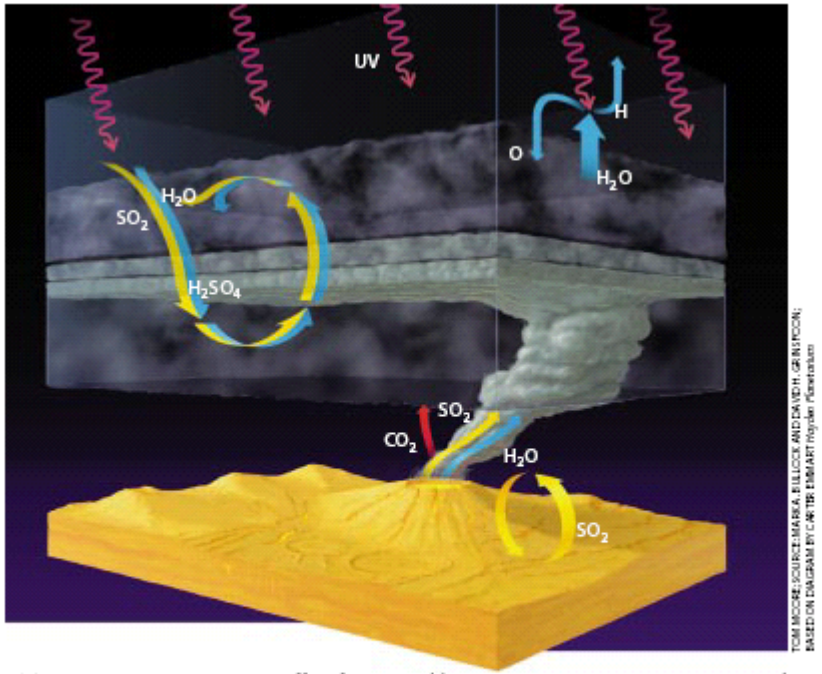

ATMOSPHERE OF VENUS suffers from ovenlike temperatures, oceanic pressures and sulfuric acid clouds (H_2SO_4). The reason is that Venus lacks the cycles that stabilize conditions on Earth. Its atmospheric processes are one-way. Carbon dioxide (CO_2), once injected by volcanoes, stays in the atmosphere; water (H_2O), once destroyed by ultraviolet light, is lost forever to the depths of space; sulfur dioxide (SO_2), once locked up in minerals, piles up on the surface (though a small amount does recycle).

Bullock, M.A. and D.H. Grinspoon: Global Climate Change on Venus. Scientific American, March 1999, 50-57.

External forcing

It is clear, however, that changes such as occurred on Venus or even Mars (Kargel and Strom, 1996) can only be explained through the interaction of solar, climate and geologic change. In the case of Mars it is speculated that substantial warming can be triggered by abrupt shifts in the tilt of the rotation axis.

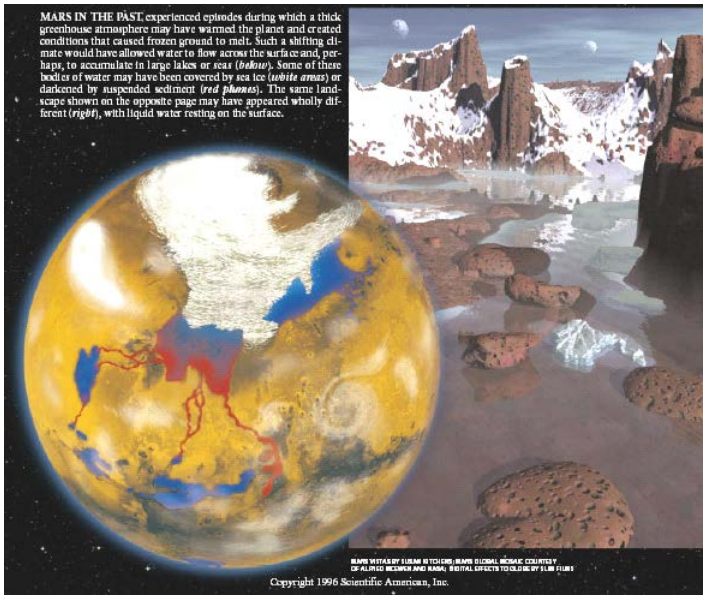

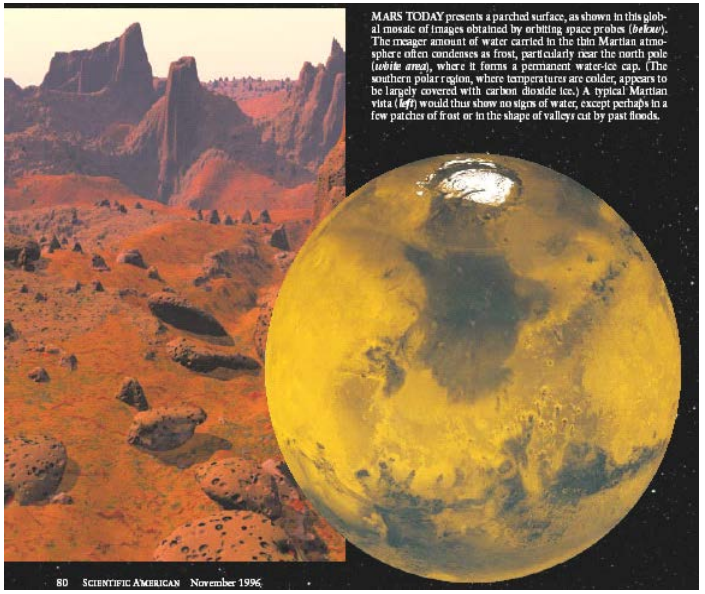

Jeffrey S. Kargel and Robert G. Strom: Global Climatic Change on Mars. Scientific American, November 1996, 80-88.

Multistates and stability in simple models

From the preceeding discussion, we conclude that the existence of multistates and the question of their stability is of relevance for the understanding the global climate system.

This kind of behaviour appears also in climate models, most notably simple energy balance models (Budyko, 1969; North, 1975), or models of the thermohaline circulation (Stommel, 1961).

We consider in the following a simple model of the global radiation balance and follow the discussion of Ghil and Childress (1987).

Budyko, M. I., 1969: The effect of solar radiation variations on the climate of the Earth. *Tellus*, **XXI** (5), 611-619.

Ghil, M. and S. Childress, 1987: *Topics in Geophysical Fluid Dynamics: Dynamo Theory and Climate Dynamics*. Applied Mathematical Sciences Vol. 60. Springer Verlag, New York, 485 pp.

North, G.R., 1975: Theory of energy balance climate models. J. Atmos. Sciences, 32, 2033-2043

Stommel, H., 1961: Thermohaline convection with two stable regimes of flow. Tellus, 13, 224.

Global radiation balance (1)

Consider the 0-dim global radiation balance

$$SW_{abs} = \frac{S_0}{4}(1-\alpha_P) = LW_{out}$$

which expresses an equilibrium between absorbed shortwave radiation (on the left) and emitted longwave radiation (on the right). Here S_0 is the solar constant and α_P the planetary albedo. We assume that:

- The planetary albedo α_P can be approximated as a stepwise function of the global temperature (see ISCCP data):

$$\alpha(T) = \begin{cases} \alpha_{ice} \approx 0.5 & \text{für} \quad T < T_L \\ \alpha = \alpha_{ice} + \dfrac{T - T_L}{T_U - T_L} \cdot (\alpha_{wat} - \alpha_{ice}) & \text{für} \quad T_L \le T \le T_U \\ \alpha_{wat} \approx 0.25 & \text{für} \quad T > T_U \end{cases}$$

Albedo parameterization

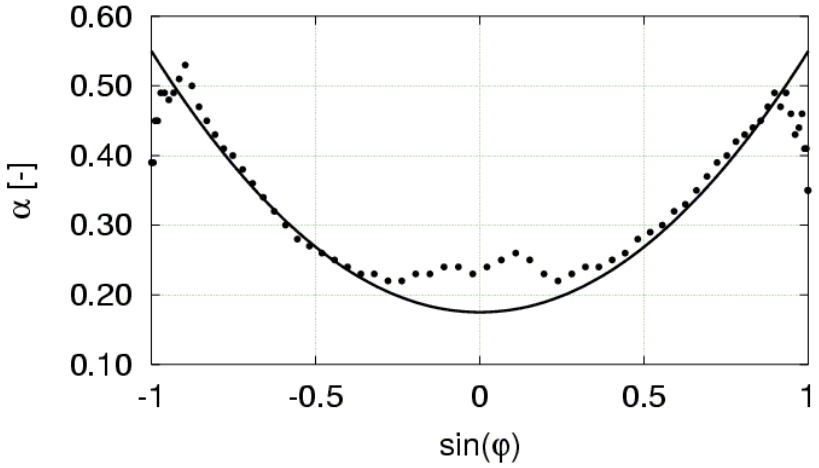

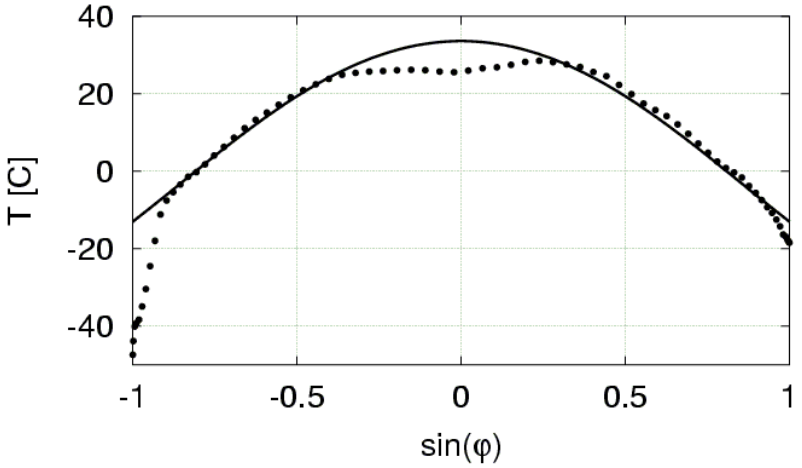

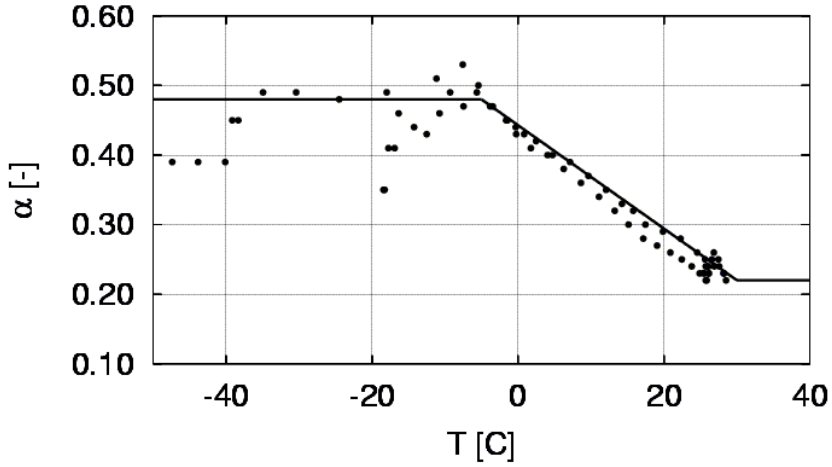

Global radiation balance (2)

- The outgoing longwave radiation, can also be approximated as a linear function of the surface temperature (Budyko, 1969):

$$LW_{out} = A + B \cdot T$$

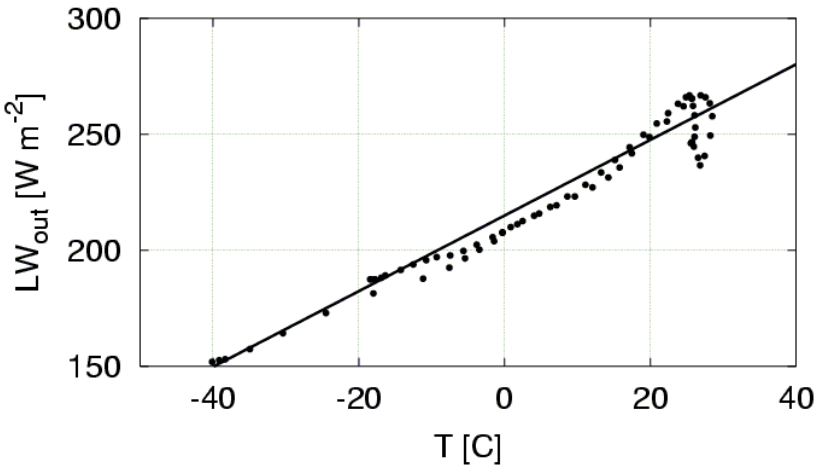

Global radiation balance (3)

At first sight this gives us the following single solution for the surface temperature:

$$T = \frac{\frac{S_0}{4}(1-\alpha_P) - A}{B}$$

However, a more careful look at a graphical solution of the problem reveals that, depending on the choice of A and B, there can exist one, two or three solutions T_1, T_2 and T_3 which, according to Ghil and Childress (1987) represent the present-day, glacial and snowball-earth states.

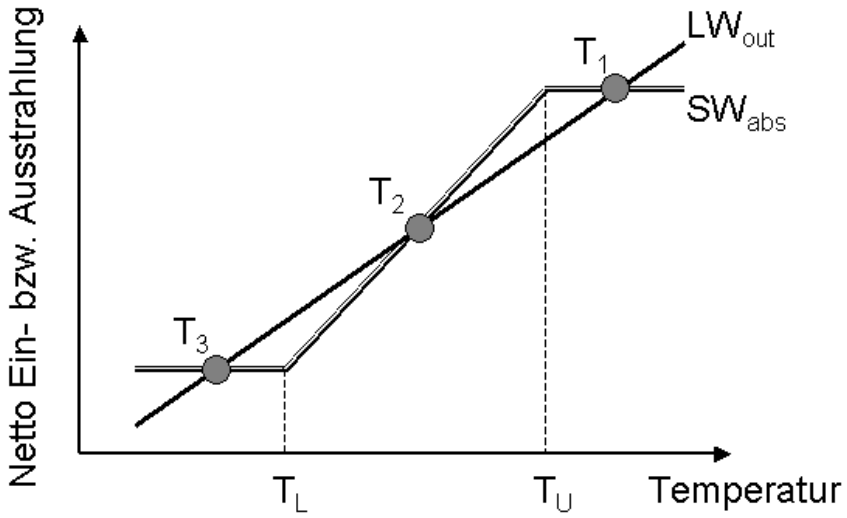

Internal stability

Not all of the solutions are stable. Let us first look at the question of the internal stability, that is the way the solution is affected by the choice of the interal parameters. Let us express $T = T_G + \theta$, where T_G is the equilibrium solution and $\theta << T_G$ a perturbation.

At T the system is not in equilibrium anymore. In this case:

$$c\frac{dT}{dt} = SW_{abs} - LW_{out} \neq 0$$

where c is the heat capacity of the system.

We now linearize the above equation (linear stability analysis) by developing:

$$SW_{abs} = SW_{abs}\Big|_G + \frac{\partial(SW_{abs})}{\partial T}\cdot\theta$$

$$LW_{out} = LW_{out}\Big|_G + \frac{\partial(LW_{out})}{\partial T}\cdot\theta$$

Internal stability (2)

We obtain:

$$c\frac{d(T_G+\theta)}{dt}=\left[SW_{abs}\big|_G+\frac{\partial(SW_{abs})}{\partial T}\cdot\theta\right]-\left[LW_{out}\big|_G+\frac{\partial(LW_{out})}{\partial T}\cdot\theta\right]$$

and because

$$c\frac{dT_G}{dt}=SW_{abs}\big|_G-LW_{out}\big|_G=0$$

we have:

$$c\frac{d\theta}{dt}=\frac{\partial(SW_{abs})}{\partial T}\cdot\theta-\frac{\partial(LW_{out})}{\partial T}\cdot\theta$$

which can be rewritten as:

$$\frac{1}{\theta}\frac{d\theta}{dt}=\frac{d\ln\theta}{dt}=\frac{1}{c}\left[\frac{\partial(SW_{abs})}{\partial T}-\frac{\partial(LW_{out})}{\partial T}\right]\equiv\lambda$$

Internal stability (3)

This is a first-order differential equation. Assuming the initial perturbation to be θ_0, we obtain the following solution:

$$\theta = \theta_0 e^{\lambda t}$$

In general, the stability condition for this system requires that the initial perturbation decays in time. If it growths, we are dealing with an unstable solution.

Mathematically we express the stability condition as:

$$\text{the solution is} = \begin{cases} \text{stable} & \text{if} \quad \lambda < 0 \\ \text{indifferent} & \text{if} \quad \lambda = 0 \\ \text{unstable} & \text{if} \quad \lambda > 0 \end{cases}$$

Internal stability (4)

In other words:

$$\text{the solution is} = \begin{cases} \text{stable} & \text{if} \quad \dfrac{\partial(SW_{abs})}{\partial T} < \dfrac{\partial(LW_{out})}{\partial T} \\ \text{indifferent} & \text{if} \quad \dfrac{\partial(SW_{abs})}{\partial T} = \dfrac{\partial(LW_{out})}{\partial T} \\ \text{unstable} & \text{if} \quad \dfrac{\partial(SW_{abs})}{\partial T} > \dfrac{\partial(LW_{out})}{\partial T} \end{cases}$$

Note that since the partial derivatives on the right-hand side represent the slope of the curves in the figure below, stability or not depends in this case on whether the curve for the absorbed shortwave radiation is less or more inclined that the curve representing the outgoing longwave radiation.

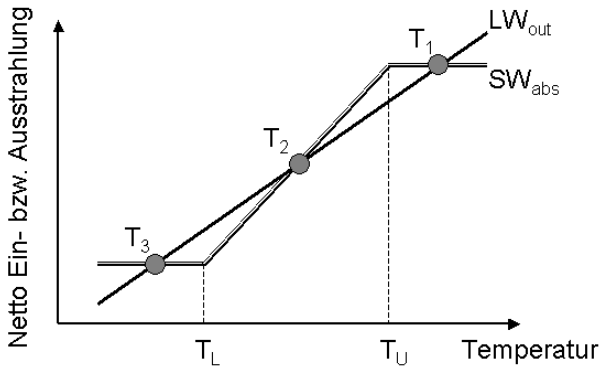

Structural stability

The second type of stability, called structural stability, refers to how the system reacts to changes in the driving variables, in this case a change in the solar constant S_0. Assuming the all other settings remains unchanged, we have the following situation:

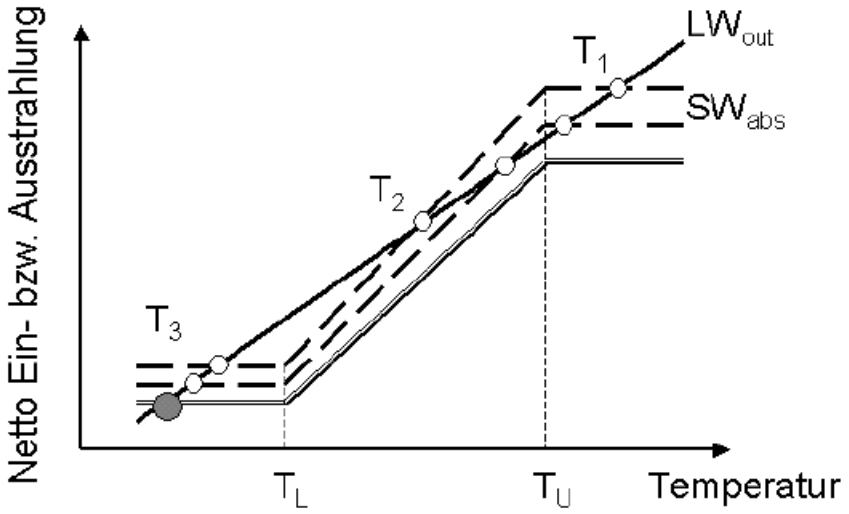

In our case, structural stability can be treated in exactly the same way as done for the internal stability. Again, stability or not of the solution depends on how the sensitivity of SW_{abs} and LW_{out} with respect to T.

Ice-albedo feedback

In the previous analysis we did not allow for changes in the planetary albedo. However, since the extent of ice masses (in particular in the northern hemisphere) is a function of temperature, changes in T induced by changes in S_0 lead to changes in the planetary albedo. We have here a beautiful example of a positive feedback, since:

decrease in $S_0 \rightarrow$ increase in $a_P \rightarrow$ decrease in $S_0 \rightarrow$ increase in $a_P \rightarrow$ ...

For small reductions of S_0, the advance of the ice masses is steadily and limited. However, when the perturbation in S_0 exceeds a critical value the system becomes unstable and we observe a sudden global glaciation, with transition to a new climatic state.

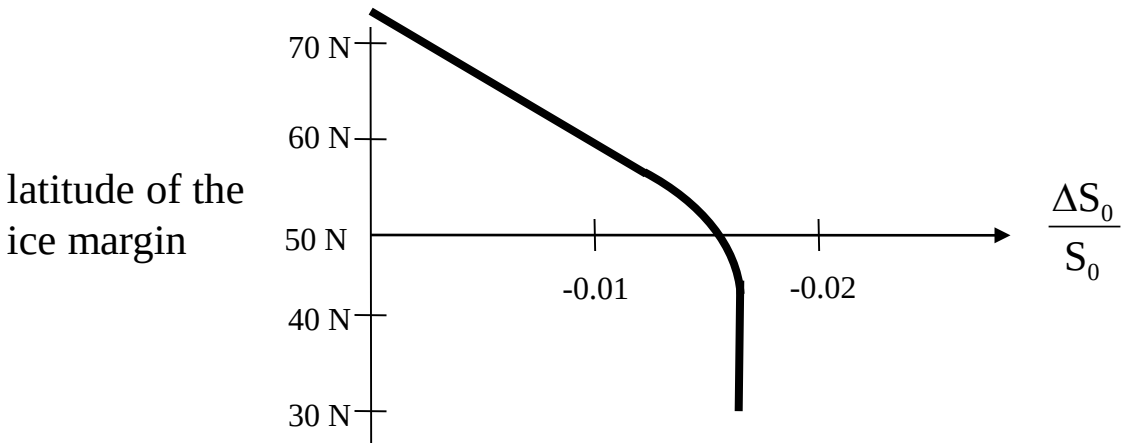

Gaia and the Daisyworld

The Gaia theory is based on the idea that plants can self-regulate the conditions (temperature) on a planet to make it more hospitable to the species which constitute "life". The theory is still highly debated, and some aspects of it are quite philosophical. But conceptually it is interesting to study its behavior. The ideas are that there are feedback loops that allow for self regulation.

To prove that such a self regulating system might indeed exist, and that is does not need any consciousness to plan and regulate, James Lovelock introduced the Daisyworld model in 1983.

Imagine a bare planet where the solar insolation is increasing over time. There are seeds for black and white daisies initially, and the ground is bare. The black daisies have a low albedo and absorb solar radiation, and they grow when it is cool. The white ones reflect radiation and therefore grow even when it’s hot. The regulatory effect is shown in the following figures.

Interestingly, the Daisyworld can also exhibit hysteresis behaviour. For certain boundary conditions, there may be two very distinct states, one without vegetation, and one full of daisies.

Gaia and the Daisyworld (II)

At the beginning, it's too cold for anything to grow. When it gets warmer, the black daisies grow and temperature increases rapidly because of the low albedo. Then, over a wide range of solar insolation, temperature is almost constant, because there is a competition between the black daisies (which prefer colder temperature) and the white ones which prefer warmer temperature). This is the self regulating effect. When the insolation is very high, nothing grows any more. Figures: Phillipa Sessini, U. Calgary.

An interesting aspect is that one can construct systems with many types of daisies, rabbits eating the daisies, foxes eating rabbits, etc. and the system can get even more stable.

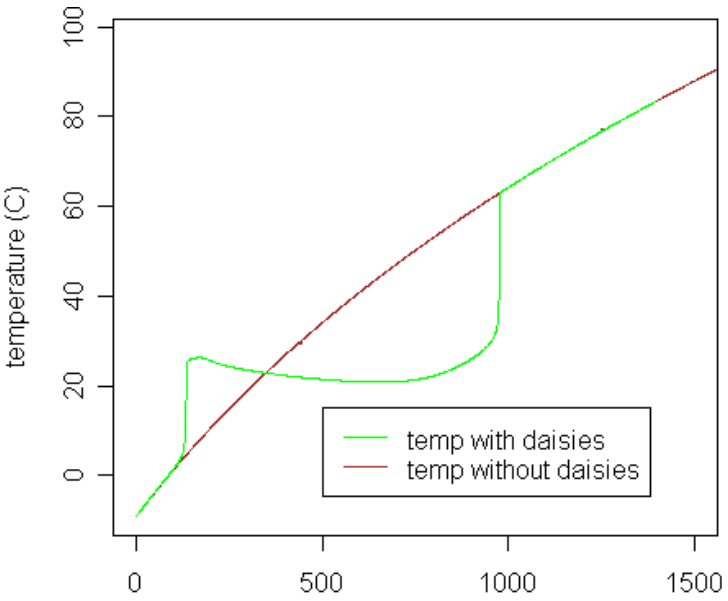

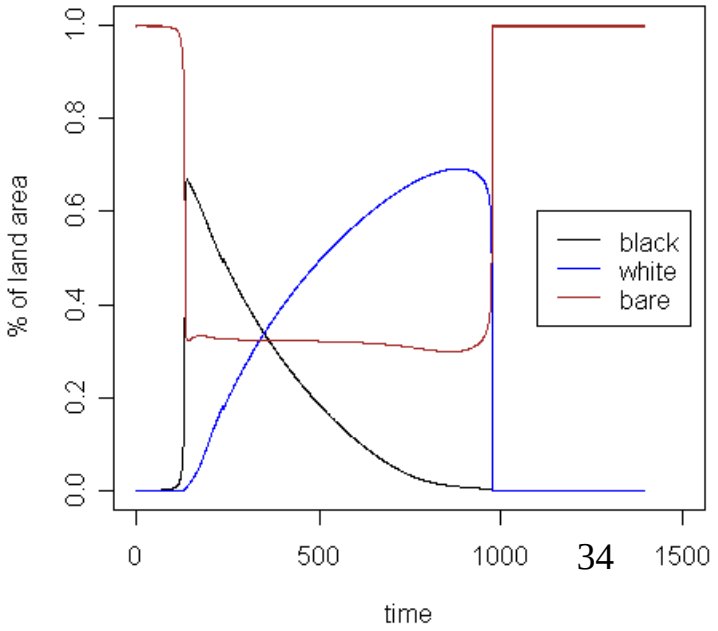

Gaia and the Daisyworld (III)

So is the Earth climate system self regulating like the Daisyworld?

There are many regulating (negative feedbacks) in the climate system. There is also hysteresis behavior. For example, if we were to remove the Greenland ice sheet today, it would probably not grow again.

For the Earth system as a whole, Richard Lindzen proposed the existence of an ‘Iris effect’: higher temperature would lead to more moisture in the air and therefore more clouds. The high albedo would cool the Earth back to near its initial state. However, studies have shown that the net effect of clouds is a positive rather than negative feedback.

Climate models show that for the future, the net feedbacks of the climate and carbon cycle feedbacks are both positive.

Climate variability

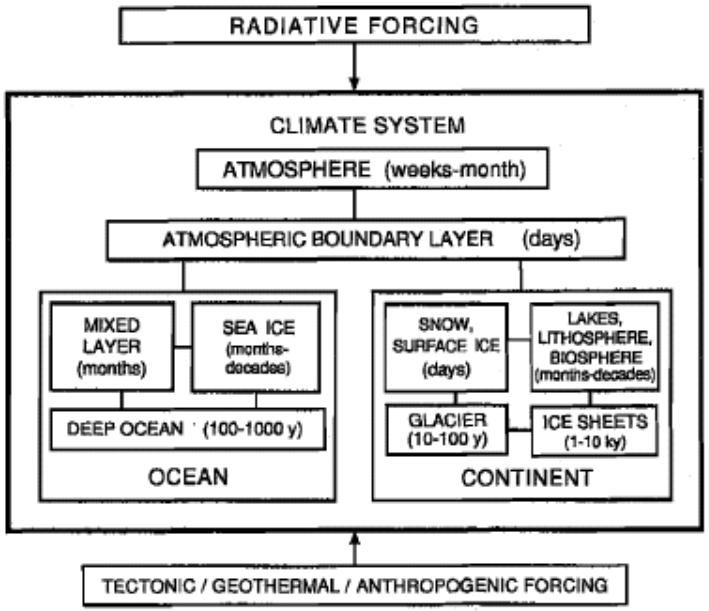

Saltzman (2002)

Figure 1-1 Schematic representation of the component domains of the internal climate system, showing their typical response time constants, and main sources of forcing.

Readings

(i) Saltzman, B., 2002, Dynamical Paleoclimatology: Generalized Theory of Global Climate Change. Academic Press, San Diego, 354 pp. (ii) Crowley, T. and North, G., 1991: Paleoclimatology. Oxford University Press, Oxford, 339 pp. (iii) Ruddimann, W.F., 2000: Earth's Climate: Past and Future. W.H: Freeman and Company, New York, 465 pp. (iv) Burroughs, W.J., 1992: Weather Cycles: Real or Imaginary? Cambridge University Press, Cambridge, 207 pp. (v) Philander, S.G., 1990: El Niño, La Niña, and the Southern Oscillation. Academic Press, London, 289 pp. ; (vi) Philander, S.G.H., 1983, El Niño Southern Oscillation phenomena. Nature, 302, 295-301. (vii) Latif, M., 2004: Klima. Fischer Verlag, Frankfurt am Main, 128 S.

Variability

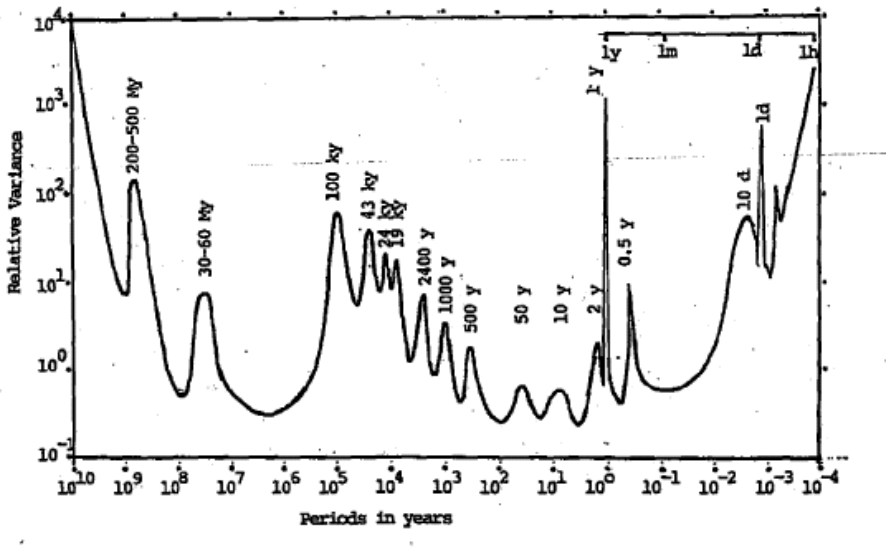

Variability of the thermal state of the atmosphere.
After Ohmura (2006)

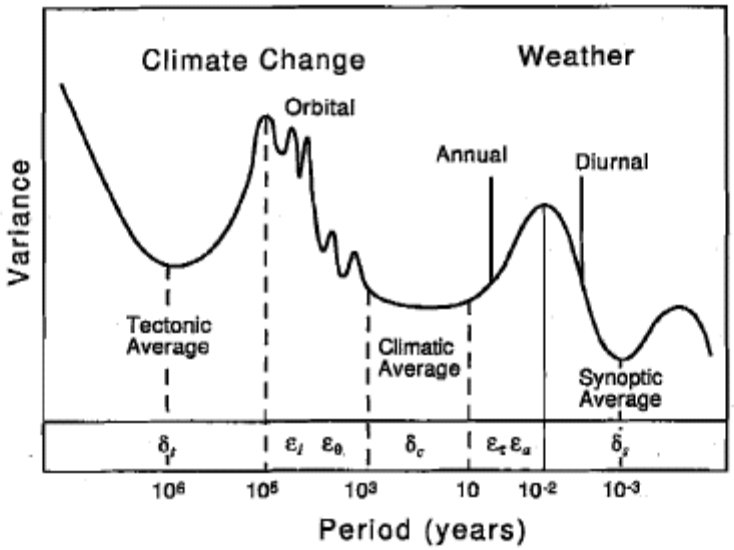

Figure 1-2 Hypothetical, highly idealized, spectrum of atmospheric thermal variance at a midlatitude point over the age of the Earth. δ_s, δ_c, and δ_t denote the synoptic, climatic, and tectonic averaging intervals, respectively, and ε_a, ε_τ, ε_θ, and ε_I denote the approximate response times for the atmosphere, oceanic mixed layer, deep ocean, and ice sheets, respectively, as will be discussed in Section 4.3.

Saltzman (2002)

Time scales

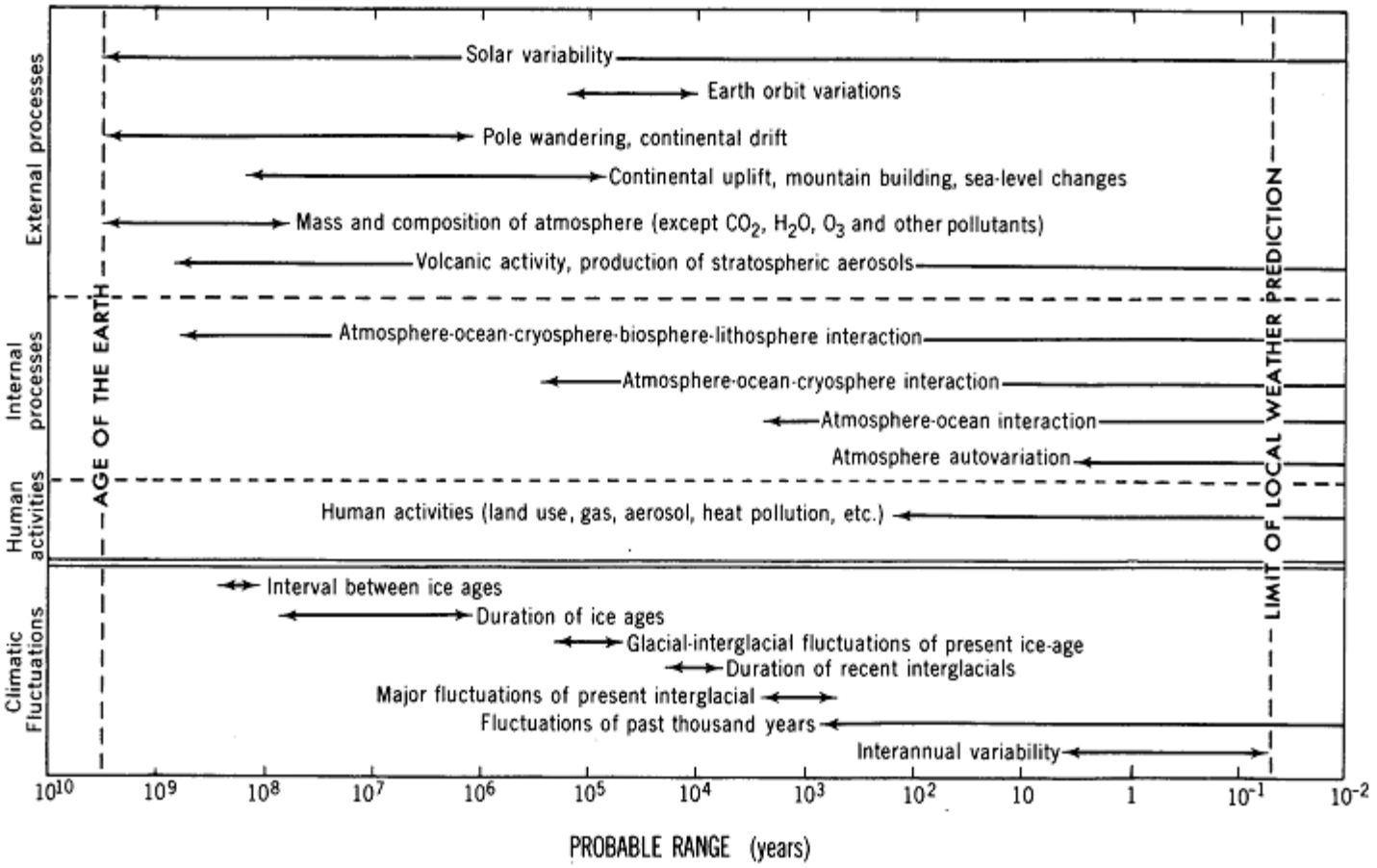

Peixoto, J. and Oort, A., 1992: Physics of Climate. American Institute of Physics, New York, 520 pp.

Formulation of the ice-age problem

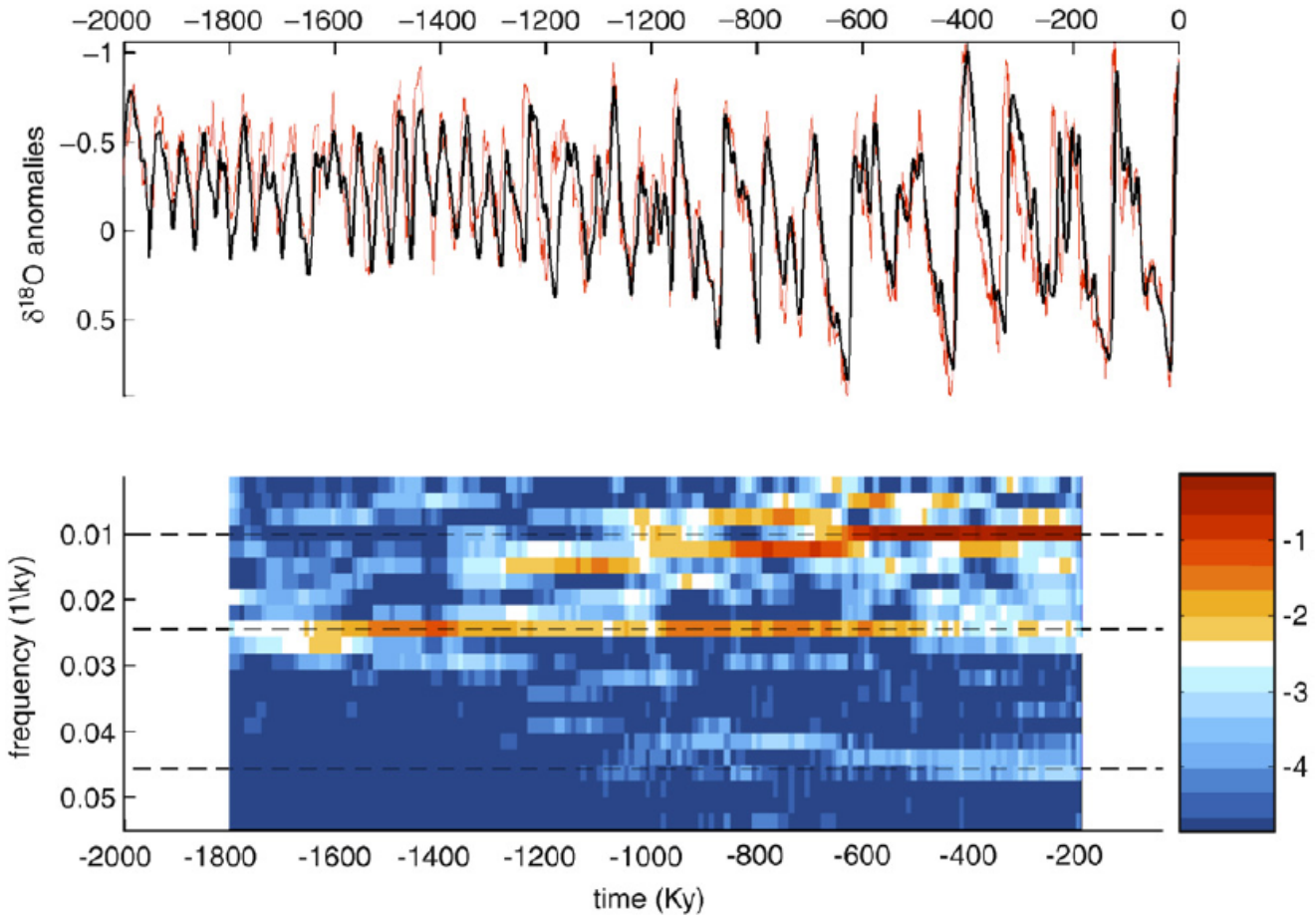

Fig. 4. Glacial variability over the last 2 Ma. The averaged δ^{18} O record is shown at top on the depth-derived agemodel (thick line). For comparison, the δ^{18} O compilation of Lisiecki and Raymo (2005) is also shown (thin line). Units are in ‰ and the mean between 700 Ka and the present has been removed. An evolutionary spectrum of the depth-derived record is shown at bottom. Shading indicates the $\log_{10}$ of the spectral power. Spectra are calculated using a 400 Ka sliding window. Horizontal dashed lines are at 1/100, 1/41, and 1/22 Ka.

Huybers QSR 2007

Formulation of the ice-age problem

For the ice-age problem, we can put down the following main questions:

- How do we explain the onset of glaciations at ~ 2 Myr before present?
- How do we explain the onset of a near 100-kyr quasi cyclic oscillation at ~ 1 Myr before present?
- How do we explain periodicities of near 20 and 40 kyr?
- Are the periodicities at near 20, 40 and 100 kyr all forced by changes in the orbital parameters?

Long-term climatic variations in insolation: Milankovitch theory

Let us fist have a look at the variation of the orbital elements (Berger, 1991). The three key elements in the orbital geometry are:

- the eccentricity, e;
- the obliquity of the earth's rotation axis relativ to the ecliptic plane, ε;
- the longitude of the perihelion, ω. The variability of e and ω induces the so-called axial precession.

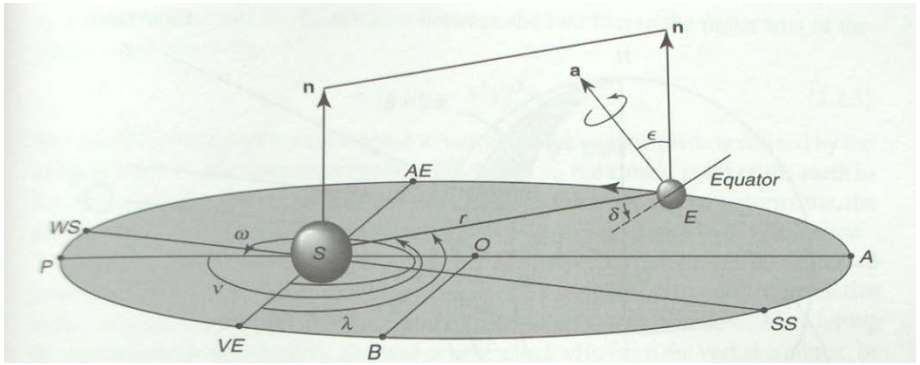

After Liou (2002)

Berger A. and Loutre M.F., 1991: Insolation values for the climate of the last 10 million years. Quaternary Sciences Review, Vol. 10 No. 4, pp. 297-317, 1991.

Long-term climatic variations in insolation (2)

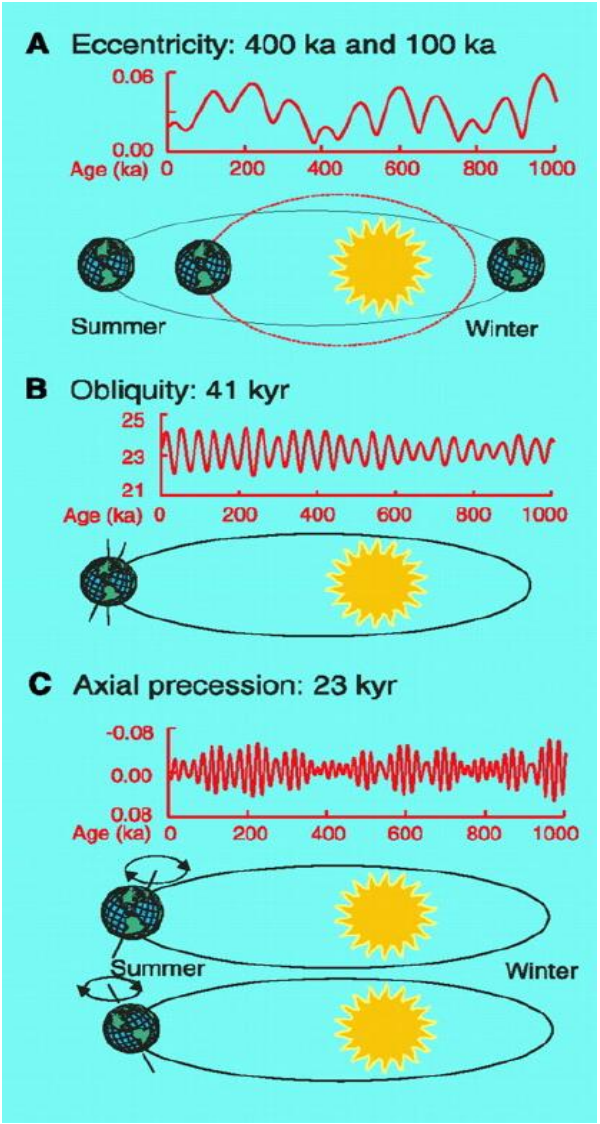

Long-term climatic variations in insolation (3)

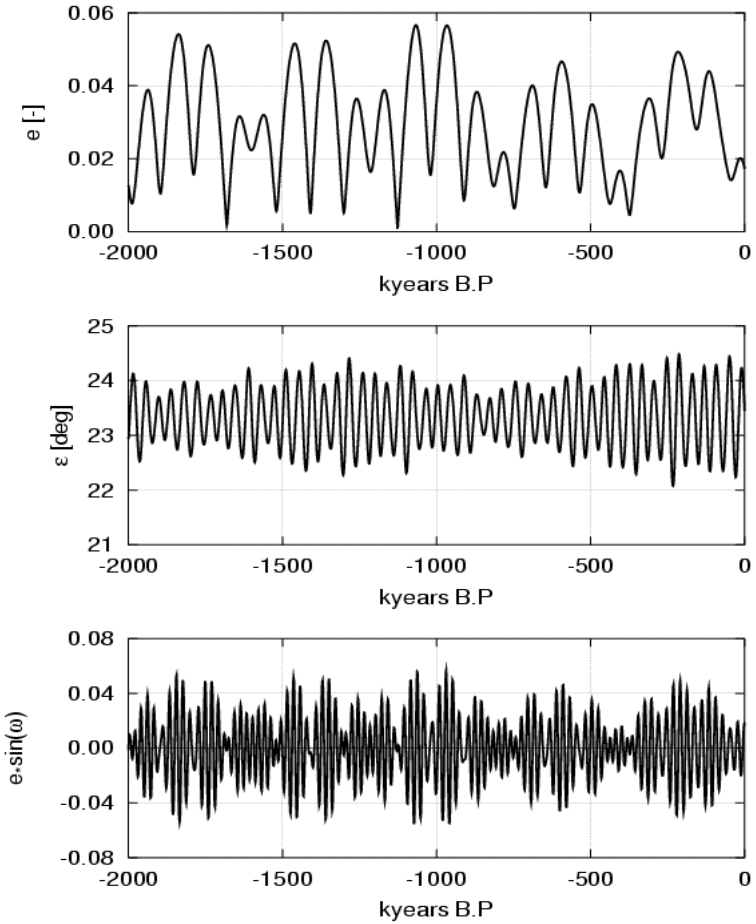

eccentricity
periodicity (P) of 100 and 413 kyr

obliquity
P of 41 kyr

precession, $e \cdot \sin(\omega)$,
P of 23 and 18 kyr

Data calculated according to Berger and Loutre (1991).

Long-term climatic variations in insolation (4)

Changes in the orbital elements give rise to changes in the insolation, which are particularly pronounced at high latitudes. Milankovitch (1941) postulated that variations in the summer insolation of the NH high latitudes (~ 65 ^{o}N) alter summer melt and affect therefore the mass balance of polar ice sheets.

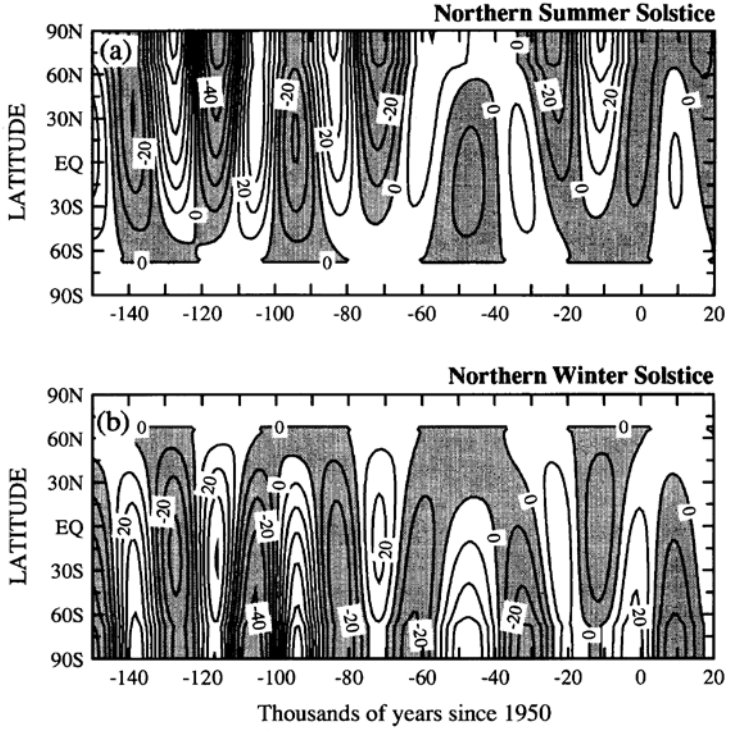

Hartmann (1994)

Milankovitch, M., 1941: Kanon der Erdbestrahlung und seine Anwendung auf das Eiszeitproblem. Beograd, Königliche Serbische Akademie.

Hartmann, D.L., 1994: Global Physical Climatology. Academic Press, San Diego.

Variability in ice-core records

The problem of dating

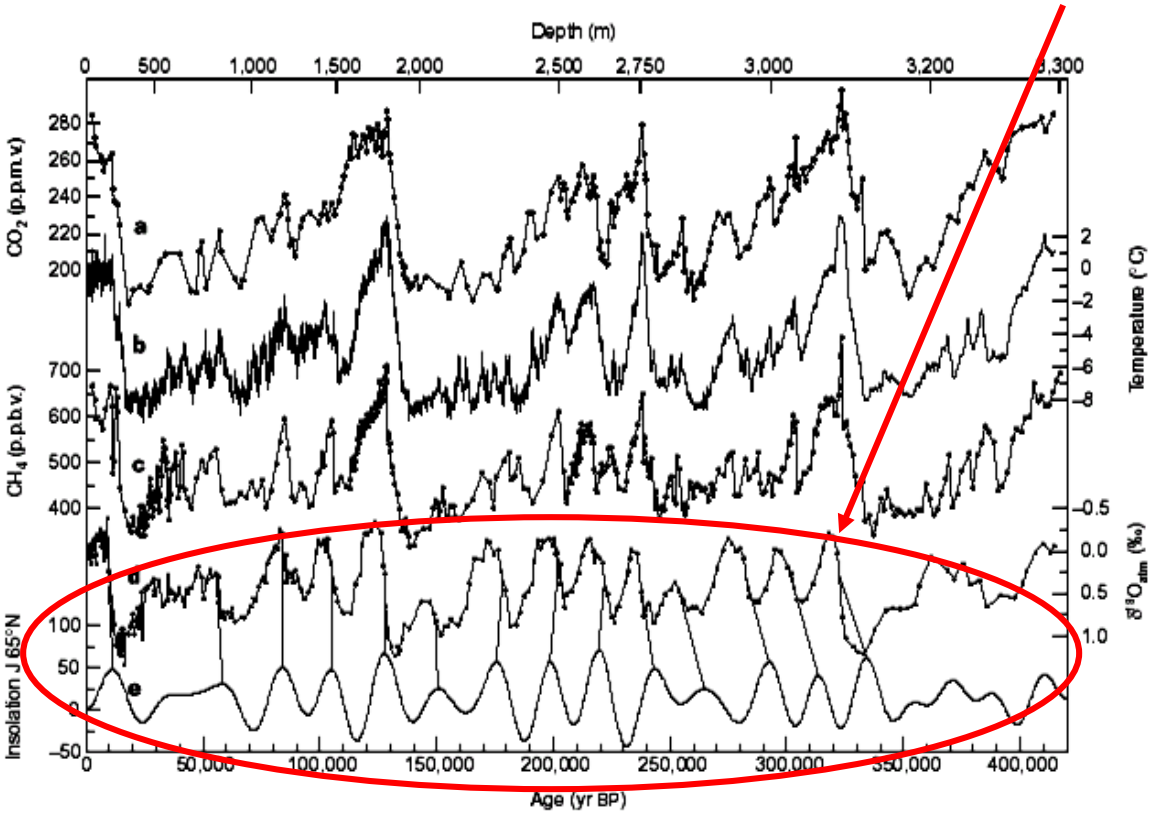

Figure 3 Vostok time series and insolation. Series with respect to time (GT4 timescale for ice on the lower axis, with indication of corresponding depths on the top axis) of: **a**, CO_2; **b**, isotopic temperature of the atmosphere (see text); **c**, CH_4; **d**, $\delta^{18}O_{atm}$; and **e**, mid-June insolation at 65°N (in Wm^{-2}) (ref. 3). CO_2 and CH_4 measurements have been performed using the methods and analytical procedures previously described[5,9]. However, the CO_2 measuring system has been slightly modified in order to increase the sensitivity of the CO_2 detection. The thermal conductivity chromatographic detector has been replaced by a flame ionization detector which measures CO_2 after its transformation into CH_4. The mean resolution of the CO_2 (CH_4) profile is about 1,500 (950) years. It goes up to about 6,000 years for CO_2 in the fractured zones and in the bottom part of the record, whereas the CH_4 time resolution ranges between a few tens of years to 4,500 years. The overall accuracy for CH_4 and CO_2 measurements are ±20 p.p.b.v. and 2–3 p.p.m.v., respectively. No gravitational correction has been applied.

Petit, J.R. et al. (1999)

Variability ice-core records (2)

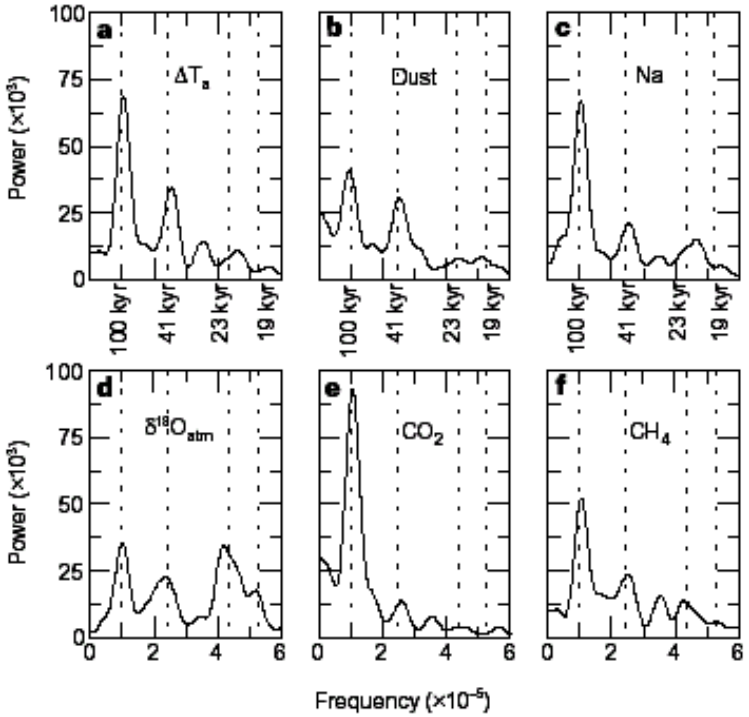

Figure 4 Spectral properties of the Vostok time series. Frequency distribution (in cycles yr^{-1}) of the normalized variance power spectrum (arbitrary units). Spectral analysis was done using the Blackman-Tukey method (calculations were performed with the Analyseries software[47]): **a**, isotopic temperature; **b**, dust; **c**, sodium; **d**, $\delta^{18}O_{atm}$; **e**, CO_2; and **f**, CH_4. Vertical lines correspond to periodicities of 100, 41, 23 and 19 kyr.

Petit, J.R. et al. (1999)

Ice cores as an example for paleo proxies

Greenhouse gas concentrations measured on polar ice core, along with local temperature (deuterium) and ice volume (oxygen isotopes) from marine cores. From IPCC (2007).

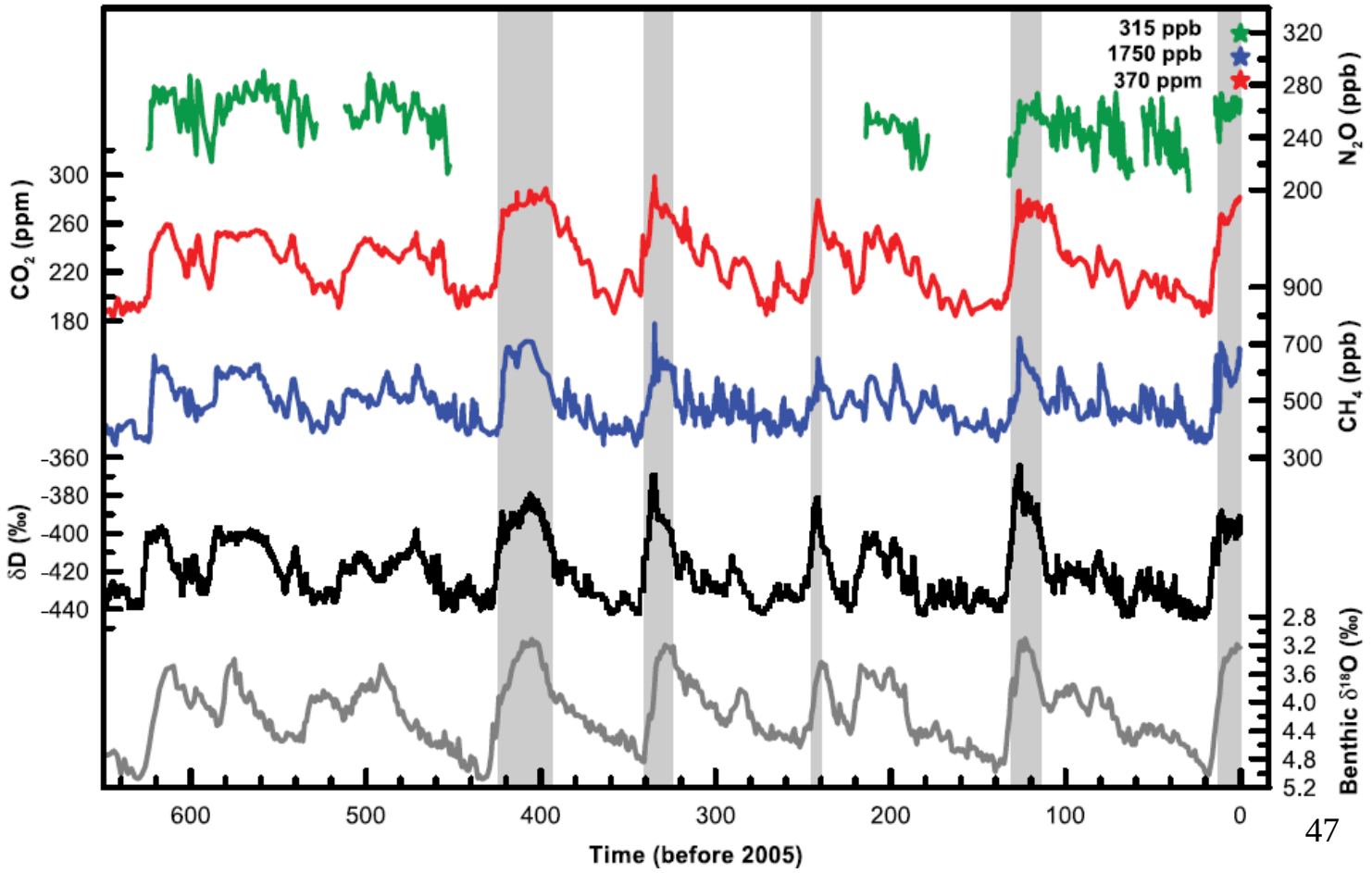

Variability in the last millennium

The was a large debate in recent years about temperature reconstructions of the millennium and the question whether the current warm phase is unusual. IPCC (2007) concluded that "it is very likely that average Northern Hemisphere temperatures during the second half of the 20th century were higher than for any other 50-year period in the last 500 years. It is also likely that this 50-year period was the warmest Northern Hemisphere period in the last 1.3 kyr." Note that question whether temperatures were as high as today a thousand years ago is meaningless without looking at the causes. Figure: global temperature reconstructions (IPCC, 2007).

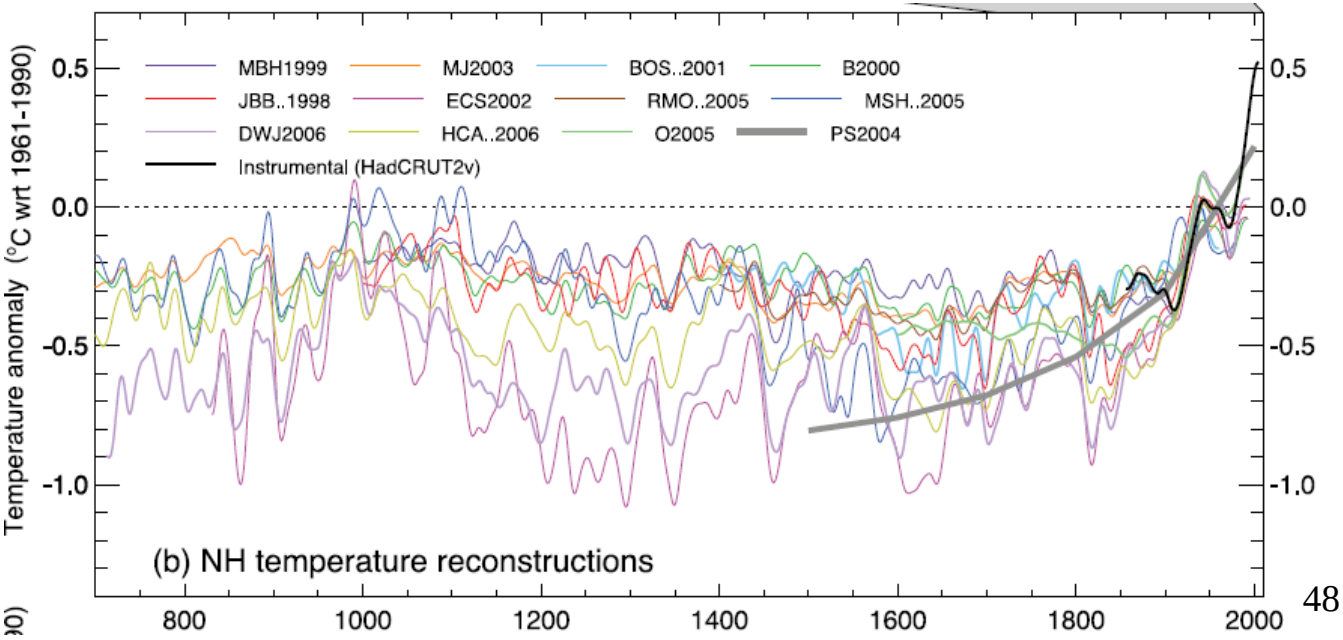

Internal unforced variability

Global temperature varies from year to year. El Nino years for example tend to be warmer than average. Internal variability can be internal and unforced (e.g. El Nino) or naturally forced (solar and volcanic. Internal unforced variability from climate models (left) is much smaller than the observed temperature trends over the last century (right). From Stouffer et al., J. Climate 2000.

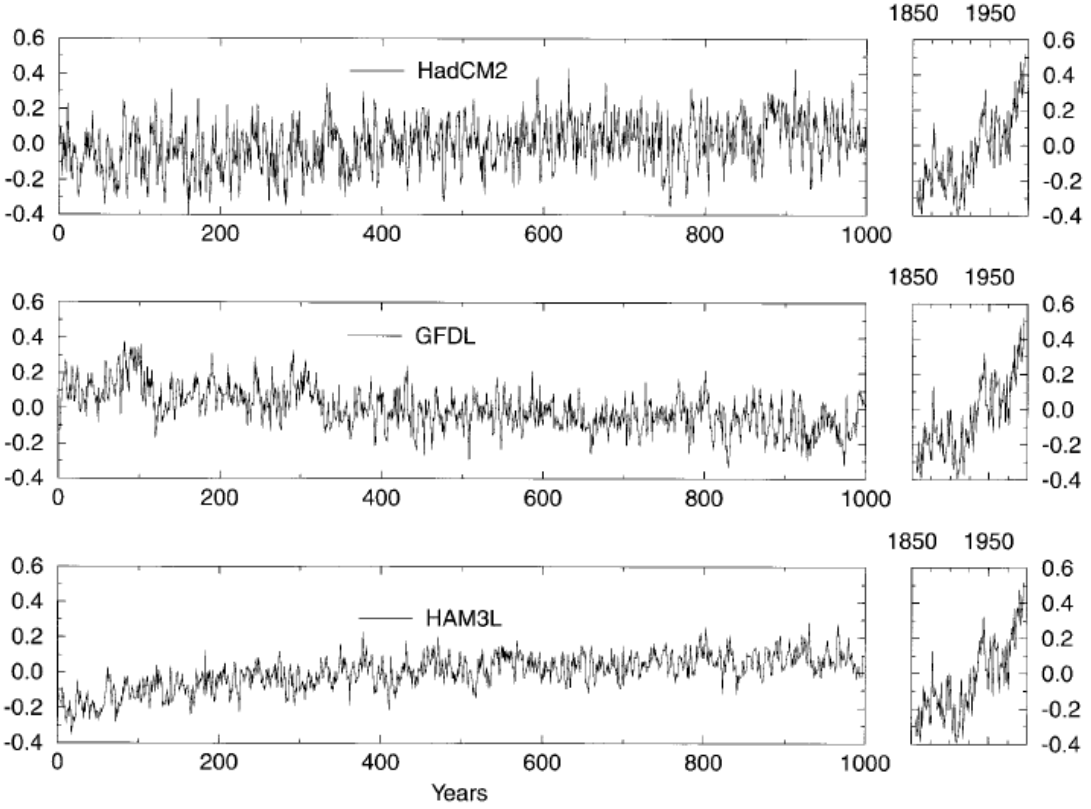

Naturally forced variability

The signal of volcanic forcing, solar forcing and greenhouse gas plus aerosols can be seen in reconstructions over the last millennium.

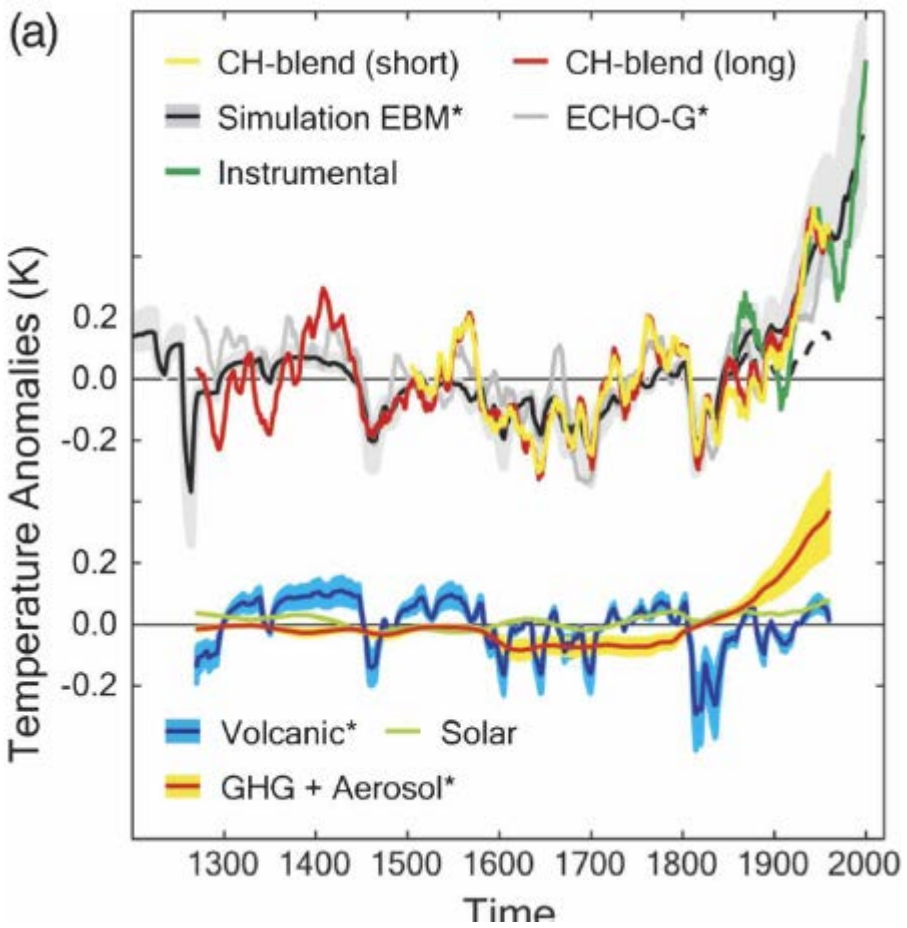

Top: Reconstructions of temperature (yellow/red) compared to model simulations (grey) and the instrumental record (green). Bottom: Contributions of external forcings to the reccontruction. From Hegerl et al. J. Climate 2007.

El Niño and the Southern Oscillation (ENSO) *

Probably the most famous and well-studied example of internal variability of the climate system on time scales ~10 years is the so-called 'El Niño Southern Oscillation' (ENSO) phenomenon (Philander, 1983).

NATURE VOL. 302 24 MARCH 1983

REVIEW ARTICLE

El Niño Southern Oscillation phenomena

S. G. H. Philander

Geophysical Fluid Dynamics Laboratory/NOAA, Princeton University, Princeton, New Jersey 08540, USA

At intervals that vary from 2 to 10 yr sea-surface temperatures and rainfall are unusually high and the tradewinds are unusually weak over the tropical Pacific Ocean. These Southern Oscillation El Niño events which devastate the ecology of the coastal zones of Ecuador and Peru, which affect the global atmospheric circulation and which can contribute to severe winters over northern America, often develop in a remarkably predictable manner. But the event which began in 1982 has not followed this pattern.

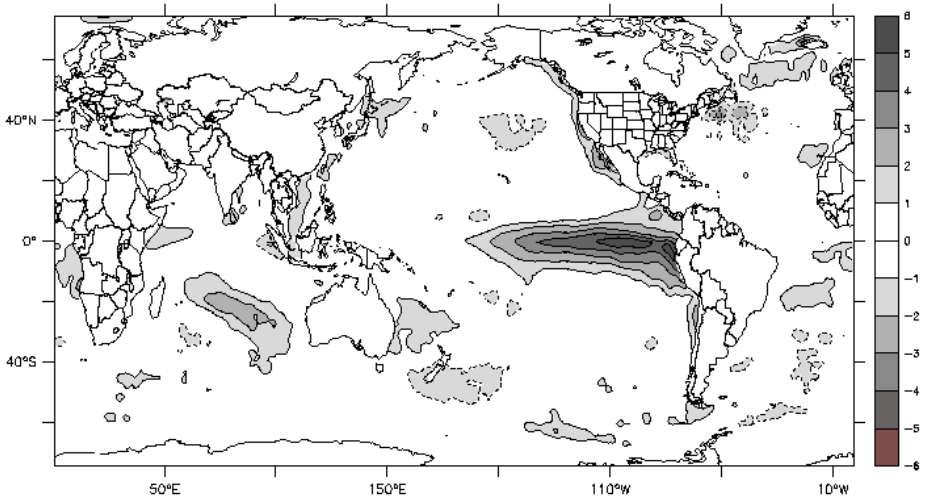

Anomaly of the sea-surface temperature in December 1997, during the 1997/1998 El Niño

The name ‘El Niño’

The name El Niño comes from the fact that a warm current flows southward along the coasts of Ecuador and Peru in Jan-Feb-Mar; the current means the end of the fishing season and its onset at about Christmas was the reason why the phenomenon was called by the local people El Niño (‘The Child’).

In some years, positive temperature anomalies are exceptionally high and persist for longer, curtailing the subsequent normal cold upwelling seasons, with distastrous consequences for the local fishers. This was for instance the case in 1982 (Philander, 1983).

Nowadays the term El Niño is associated to these more dramatic events.

Oceanic currents

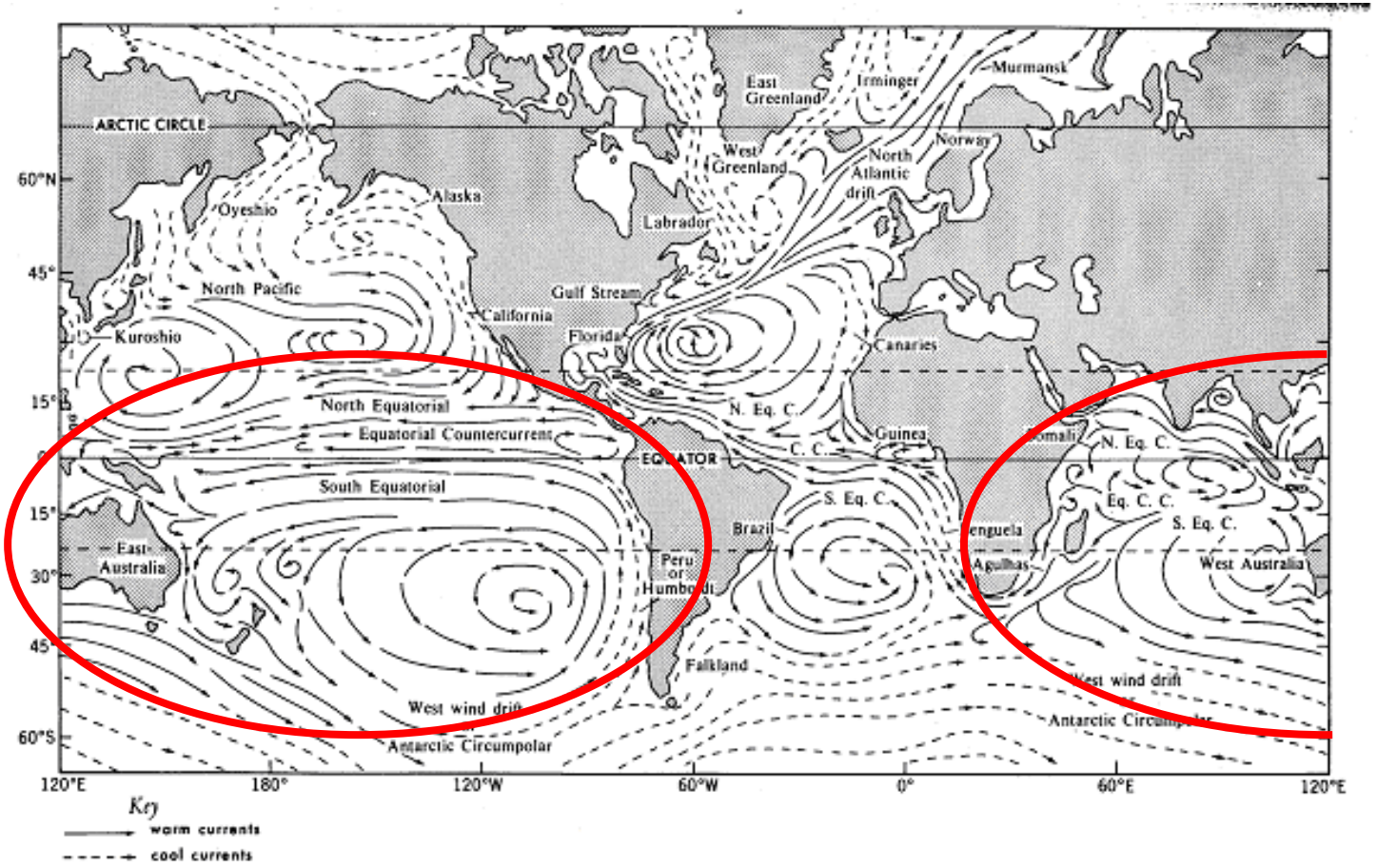

From Trenberth, K.E., 1992: *Climate System Modeling*, Cambridge University Press, Cambridge, 788 pp. (p. 123)

El Niño and La Niña

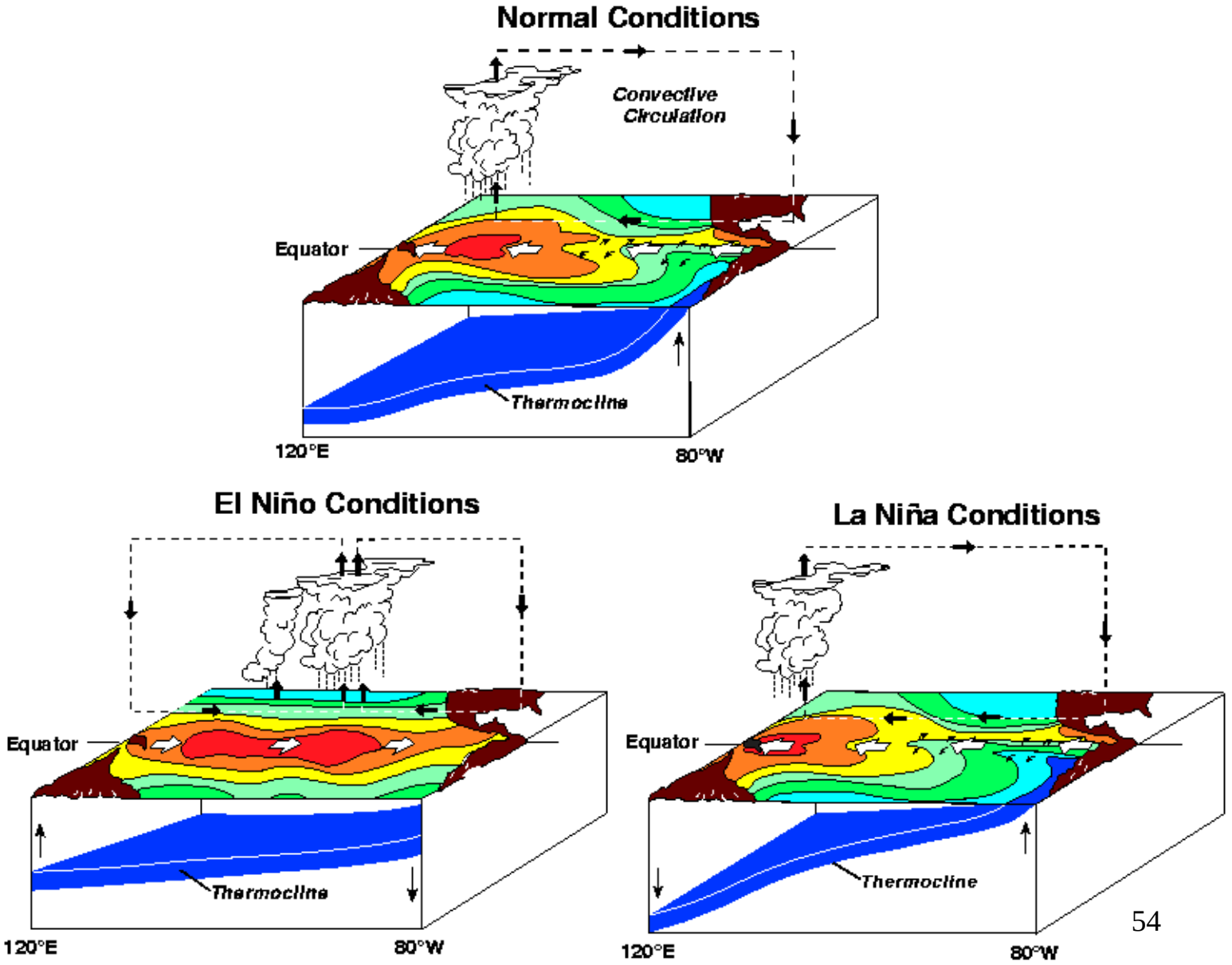

The Southern Oscillation

The discover of the Southern Oscillation is due to Sir Gilbert Walker (papers published in the 1920s and 1930s), who found that ‘when pressure is high in the Pacific Ocean, it tends to be low in the Indian Ocean from Africa to Australia.’ The associated circulation is know called Walker circulation.

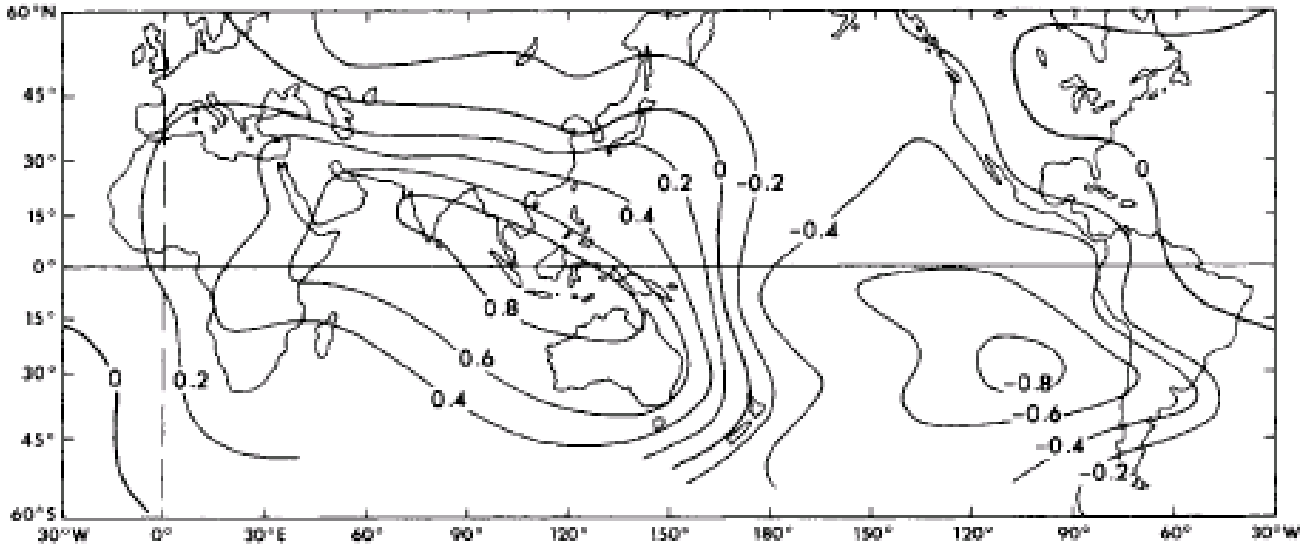

Fig. 1 The correlation of monthly mean surface pressure with that of Djakarta[45]. The correlations are large and negative in the South Pacific High Pressure Zone and are large and positive in the Australian–Indonesian Low Pressure Zone. The SO is not a standing oscillation so that correlations do not have a maximum at zero lag[46,47].

Philander (1983)

The Southern Oscillation (2)

The map shows that the SO is a barometric record of exchange of atmospheric mass along the complete circumference of the globe in tropical latitudes. Based on the pressure difference between the two centers of the previous map (Darwin and Easter Island) one can construct the so-called Southern Oscillation Index (SOI).

The standard view about periodicities in the SO is that while it has an average period of ~ 3 years, it is irregular in nature, as seen in the time series of the SOI (next page).

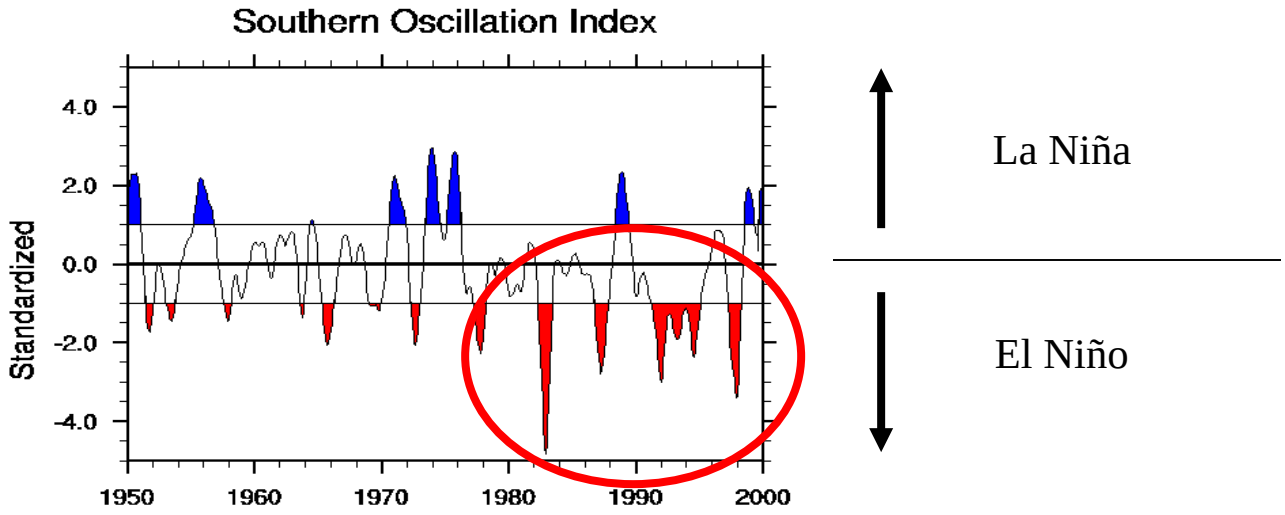

Atmospheric-oceanic interactions

The links between atmospheric patterns (Southern Oscillation) and large-scale fluctuations on the surface temperature of the tropical Pacific (El Niño) are the key to ENSO.

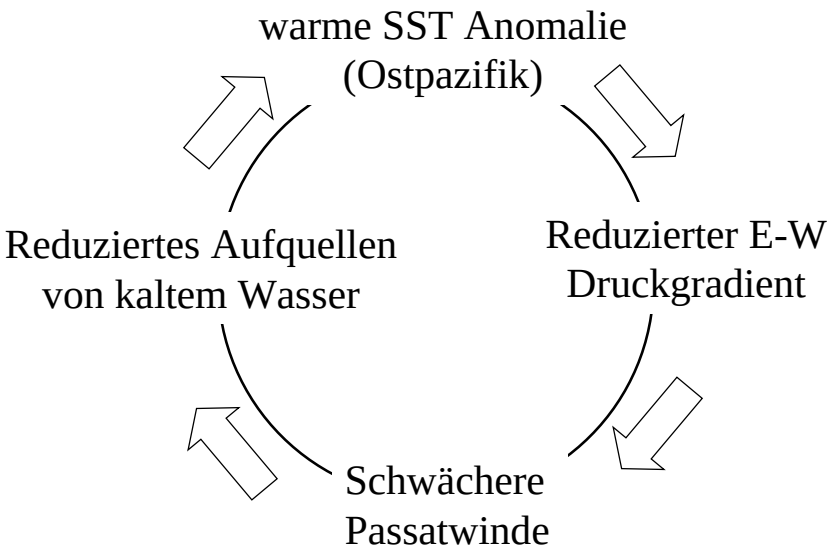

Impacts of El Niño

The following figures shows the impact of the 1997/98 El Niño.

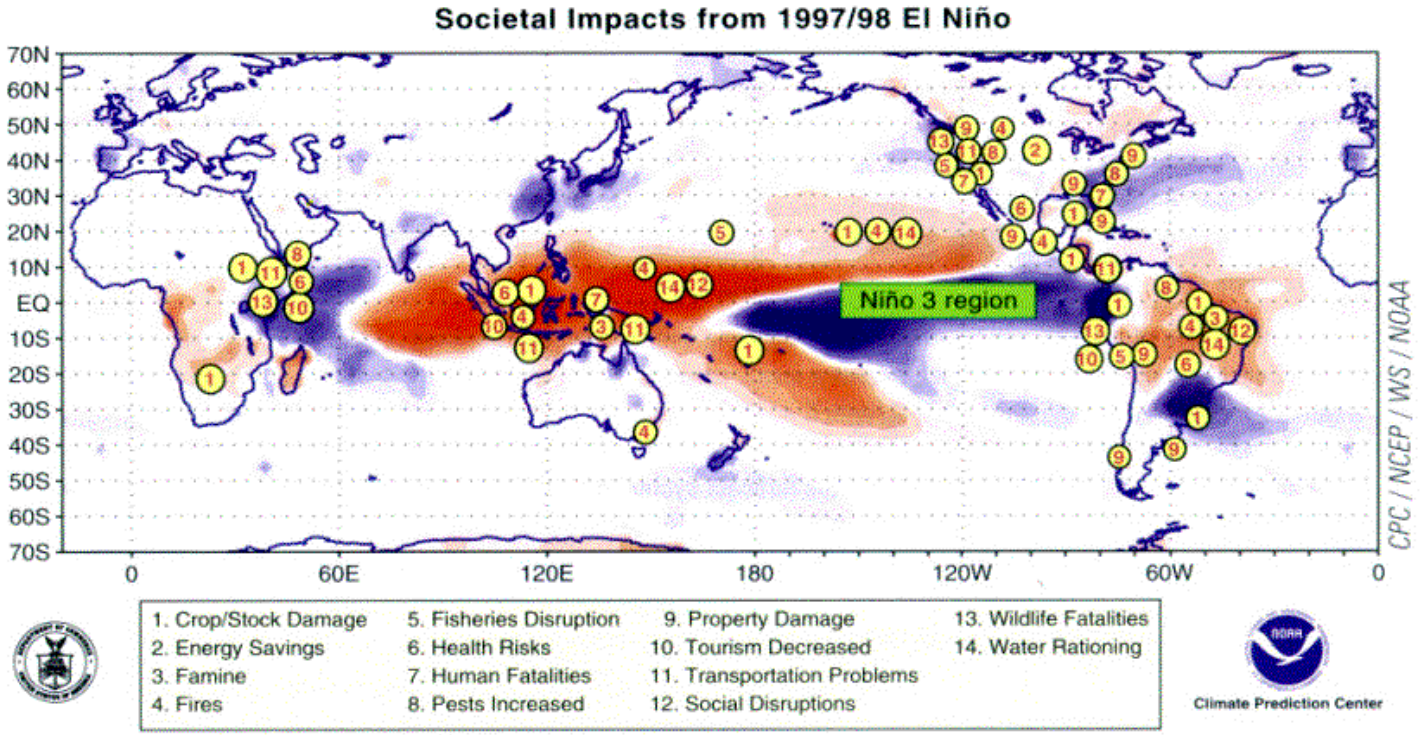

Red: rainfall below normal, blue: rainfall above normal. Compare the observed rainfall pattern with that predicted by the coupled ocean-atmosphere model; see page 23.

Courtesy of NOAA (Climate Prediction Center)

A typical El Niño

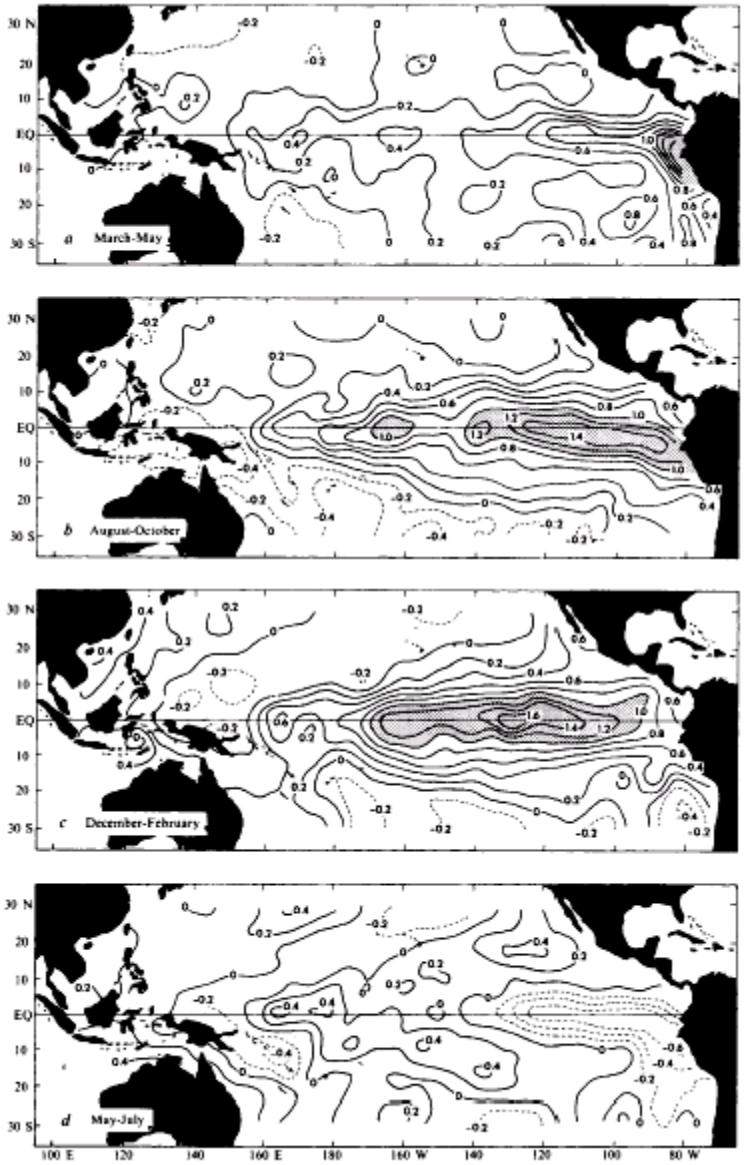

Fig. 3 Sea-surface temperature anomalies (in °C) during a typical ENSO event obtained by averaging data for the events between 1950 and 1973. *a*, March, April and May after the onset; *b*, the following August, September and October; *c*, the following December, January and February; *d*, May, June and July, more than a year after the onset[12].

Philander (1983)

A sequence of events

The events associated to a typical El Niño are:

- prior to the onset of a El Niño changes in the large scale atmospheric circulation patterns, with an increase in pressure over the western Pacific and associated weakening of the trade winds west of the dateline.
- shift of the ITCZ toward the south;
- during the mature phase, westward expansion of anomalous conditions. very weak trade winds. This phase is highly predictable;
- besides changes in the atmosphere, changes in the oceanic settings occur. Due to very weak trade winds, sea level in the western Pacific falls and the depth of the thermocline is reduced;
- intense eastwards oceanic currents between the equator and 10 ^{o}N carry warm waters away from the west Pacific (this is the reason for the apparent westward propagation of the positive sea surface temperature anomaly);
- along the western coast of the Americas there is an increase in sea level that propagates polewards in both hemispheres. This motion creates an eastward propagating Kelvin wave;
- return to normal conditions: the amplitude of the anomalous conditions off the coast of South America returns to normality a few months after the onset of El Niño.

ENSO teleconnections

WARM EPISODE RELATIONSHIPS DECEMBER - FEBRUARY

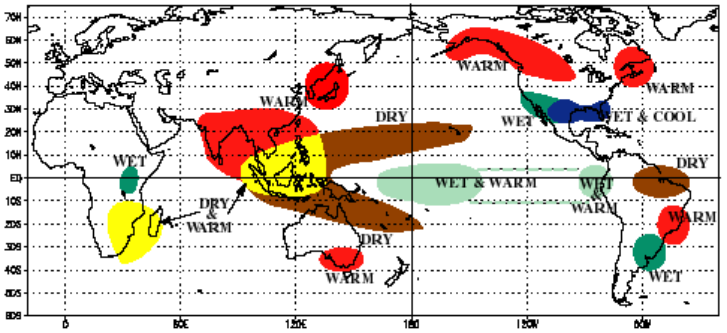

COLD EPISODE RELATIONSHIPS DECEMBER - FEBRUARY

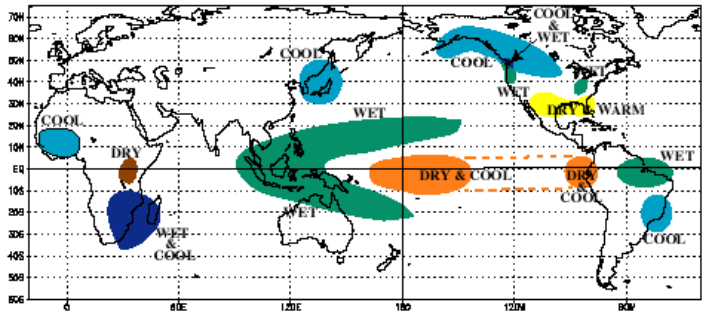

WARM EPISODE RELATIONSHIPS JUNE - AUGUST

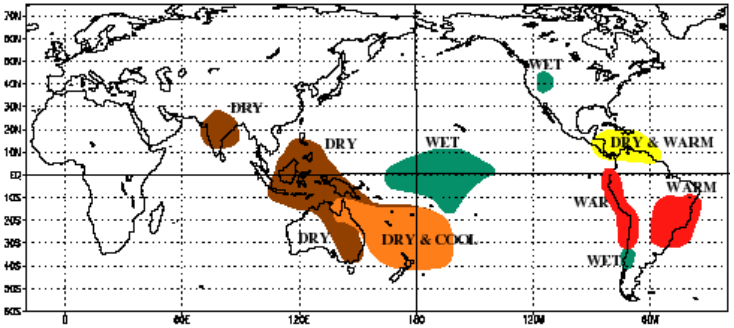

COLD EPISODE RELATIONSHIPS JUNE - AUGUST

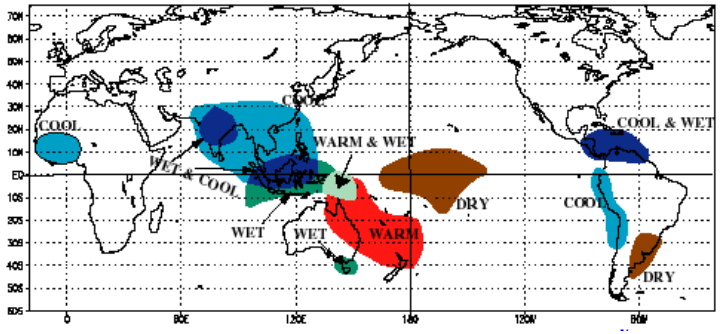

ENSO forecasts: an example from April 2009

The NCEP CFS ensemble mean (heavy blue line) predicts La Niña will end during April 2009, followed by positive SST anomalies in the Niño 3.4 region during the last half of 2009.

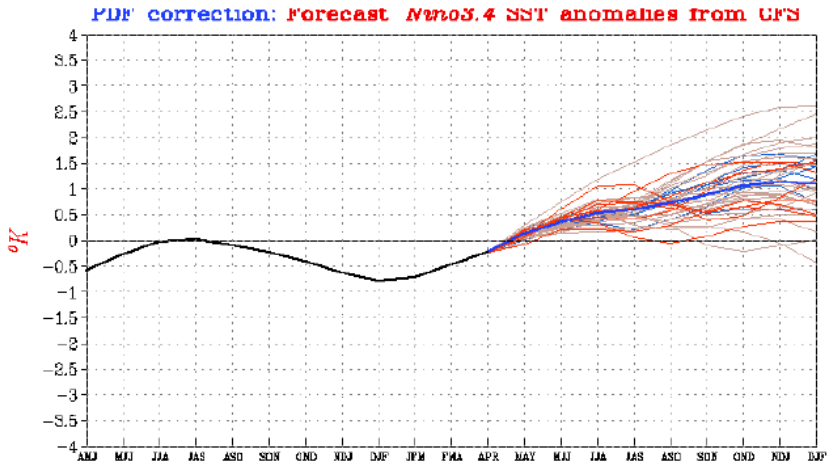

May-July 2009 outlooks indicate warmer and dryer than average conditions in the US South West.

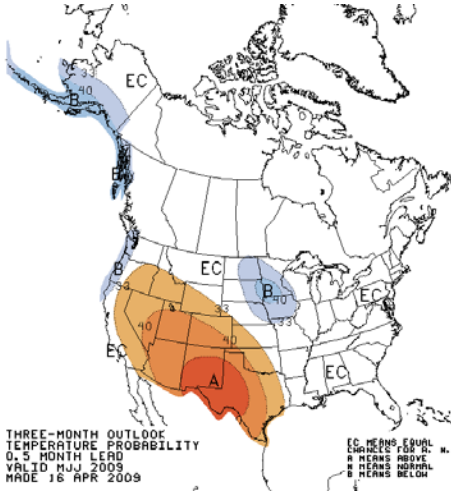

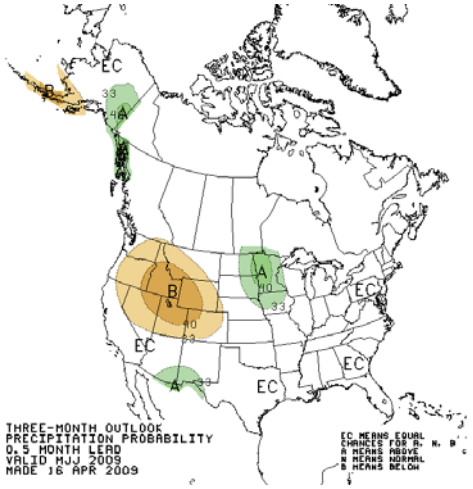

http://www.cpc.noaa.gov/products/analysis_monitoring/lanina/enso_evolution-status-fcsts-web.pdf

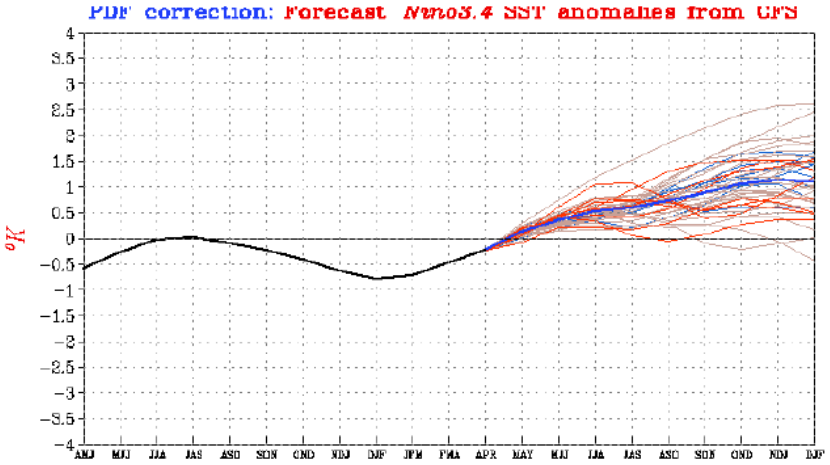

Forecast

Verification

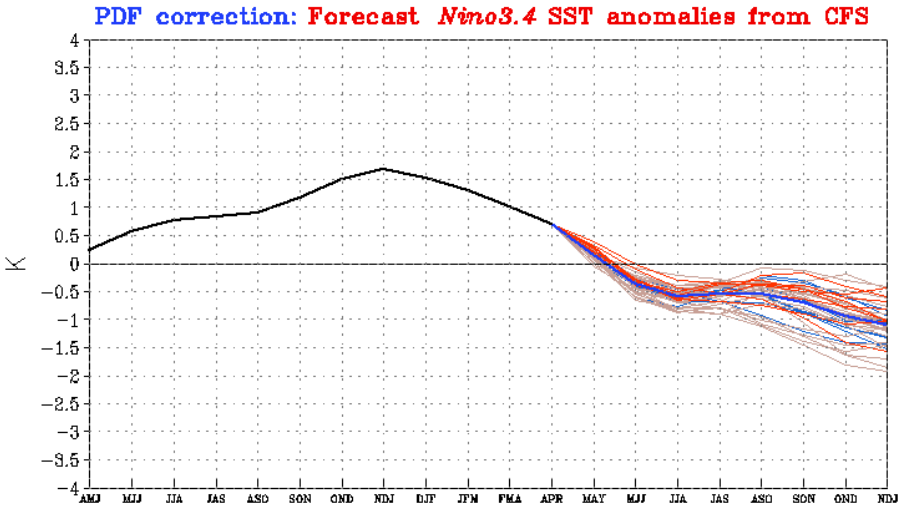

http://www.cpc.noaa.gov/products/analysis_monitoring/lanina/enso_evolution-status-fcsts-web.pdf

ENSO in climate models

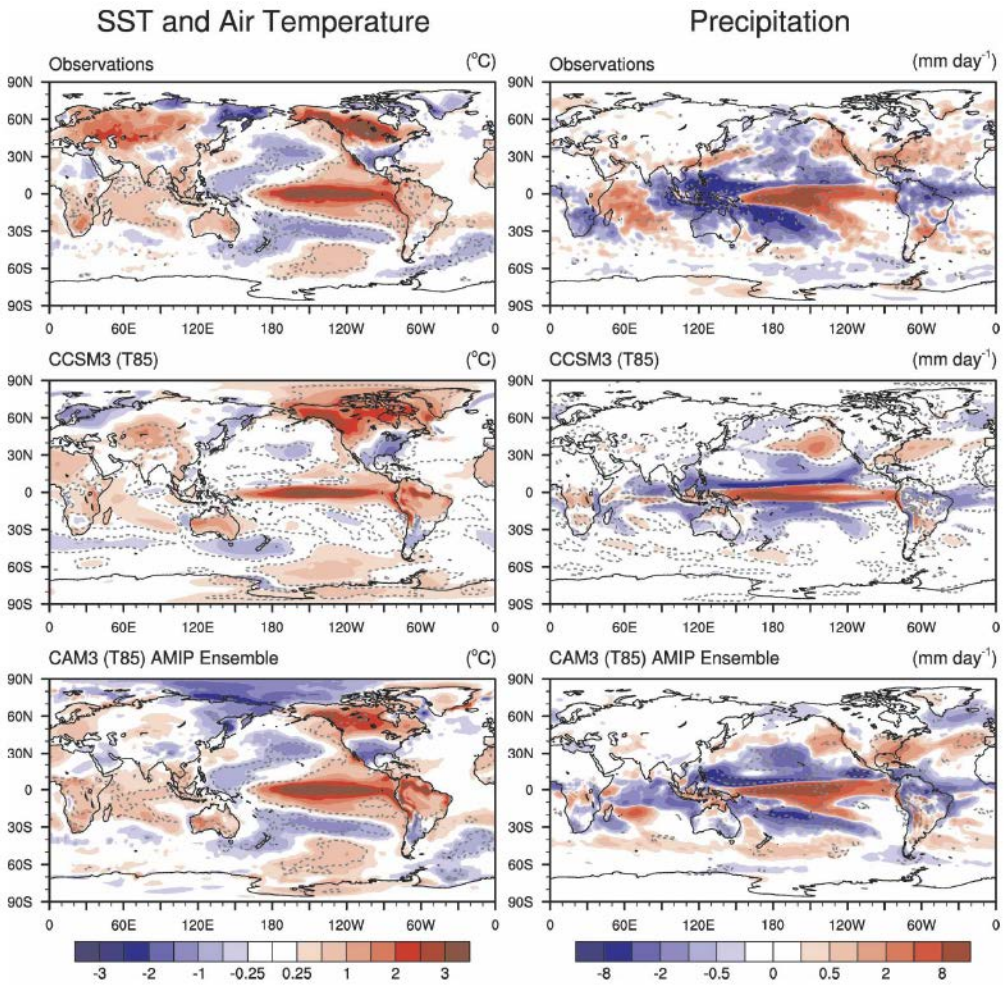

Temperature and precipitation anomalies (warm – cold event) for ENSO Dec-Jan from observations (top) . Coupled ocean atmosphere models (here CCSM3 as an example) capture part of the pattern (middle). Atmospheric models with prescribed ocean conditions (bottom) agree much better with observastions. From Deser et al., J. Climate 2006.

The North Atlantic Oscillation

The NAO index is defined as the anomaly in pressure difference between the polar low and the subtropical high in the boreal winter season. A positive NAO means a more pronounced low over Iceland and high over the Azores. The larger gradient leads to more and stronger storms on a more northerly track and to warm and wet winters in Northern Europe.

Positive NAO

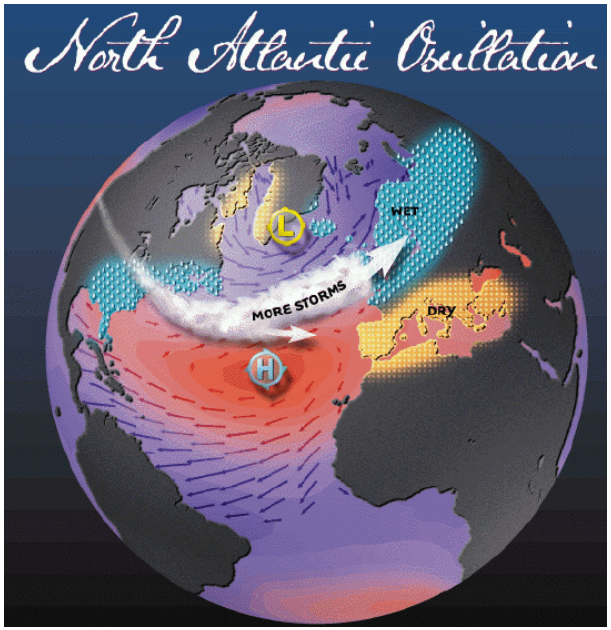

Negative NAO

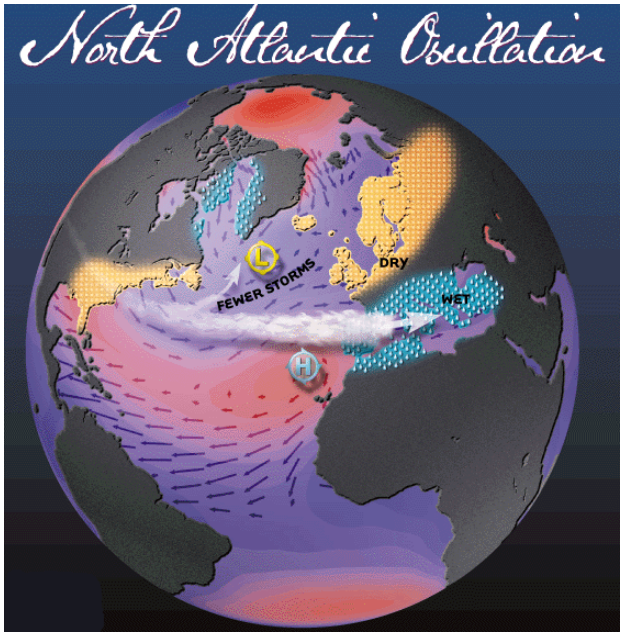

http://www.ldeo.columbia.edu/res/pi/NAO/

The North Atlantic Oscillation

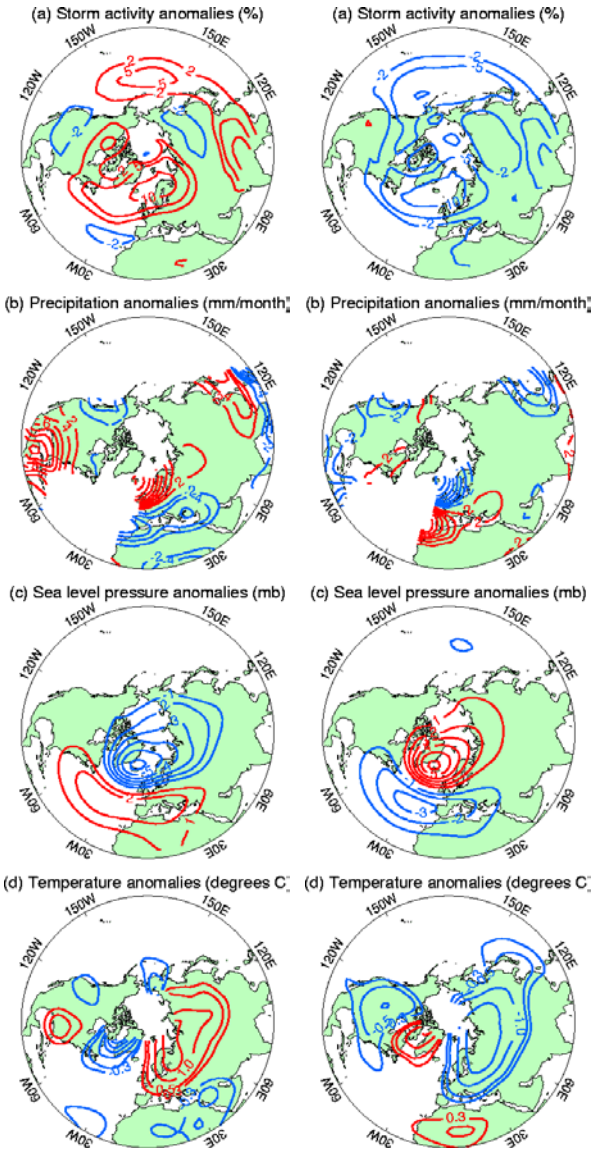

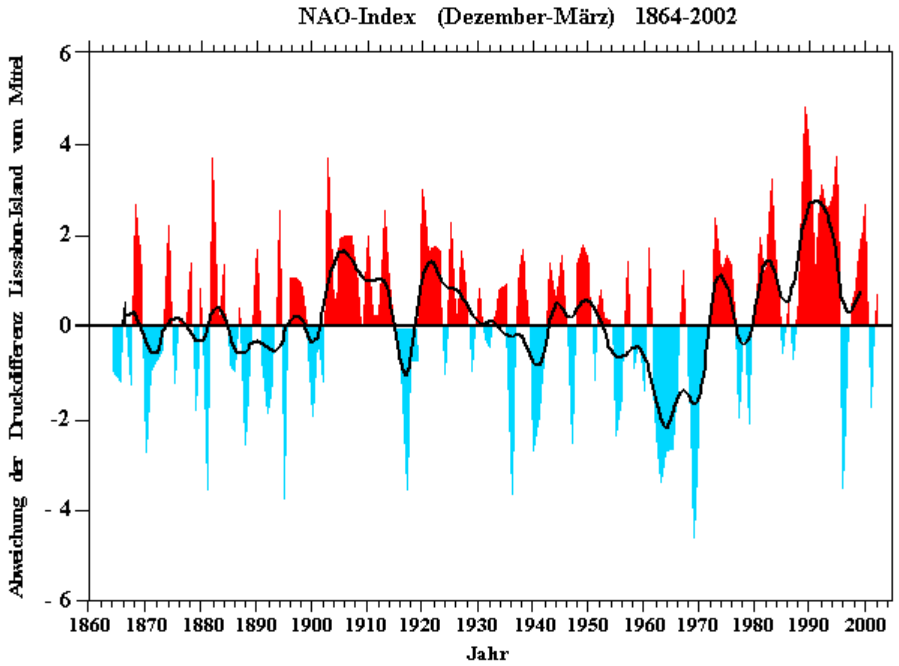

http://www.cru.uea.ac.uk/cru/info/nao/
http://www.hamburger-bildungsserver.de/welcome.phtml?unten=/klima/klimawandel/atmosphaere/nao2.html

The North Atlantic Oscillation

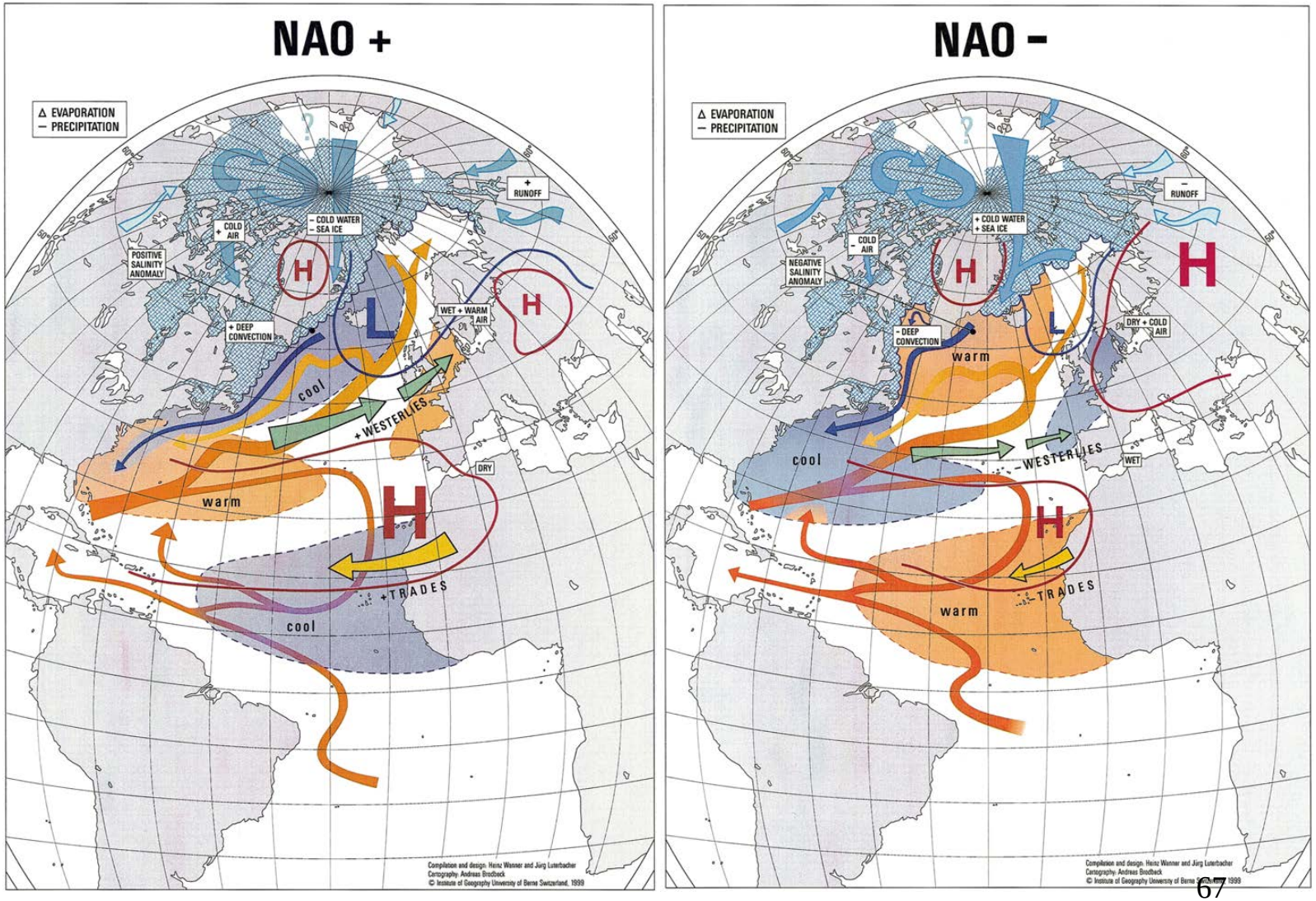

(Wanner et al. 2002)

Other modes of variability

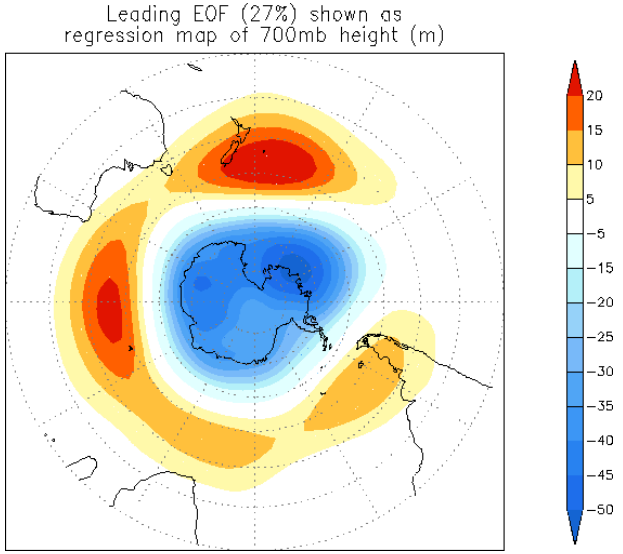

There are many other modes of variability in the coupled ocean atmosphere system, which operate on timescales of a few years. These are often observed but not well understood. They make the detection of anthropogenic influence on climate more difficult than if the fluctuations around the forced trends were purely random.

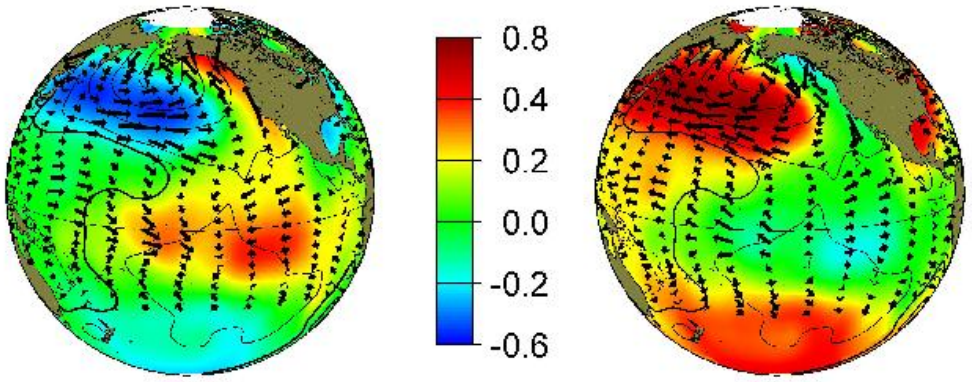

Examples: Southern Annular Mode (top, geopotential height) and Pacific Decadal Oscillation (bottom, temperature in color and pressure in contours)

(http://www.jisao.washington.edu/pdo/)